2020

Tidal Power Optimization Using Two Bladder System

Binita Yadav
University of North Florida, n01423076@unf.edu

TIDAL POWER OPTIMIZATION USING TWO BLADDER SYSTEM

By

Binita Yadav

A Thesis submitted to the Department of Civil Engineering

in partial fulfillment of the requirements for the degree of

Master of Science with Major in Coastal and Port Engineering

The University of North Florida

College of Computing, Engineering and Construction

July 2020

Chairperson of the Supervisory Committee

Dr. Cigdem Akan

Department of Civil Engineering

Members of the Supervisory Committee

Dr. Don Resio

Department of Civil Engineering

Dr. John Nuszkowski

Department of Mechanical Engineering

The thesis of Binita Yadav is approved by:

Dr. Cigdem Akan, Committee Chair	Date
Dr. Don Resio, Committee Member	Date
Dr. John Nuszkowski, Committee Member	Date

Abstract

The kinetic and potential components of tidal energy can be utilized to generate electricity.The system discussed in the paper utilizes a head difference in generating electricity.This thesis presents the research work on the optimization of the nozzle, which will be used in a Closed Tidal Energy Conversion System for generating electricity. For this purpose, the relatively small-scale numerical simulation of the flow through the nozzle with 10 inches inlet diameter was executed using a computational fluid dynamics software, ANSYS. The inlet diameter and the length of the nozzle were kept constant, and the outlet diameters used are 7.5 inches, 6 inches, 5.75 inches, 5 inches, 4 inches, and 3 inches. The results showed that the nozzle with 10 inches outlet diameter and 5.75 inches inlet diameter set forth the desired velocity of this system, i.e., approximately 10 m/s. Also, it is assumed that the system holds the static pressure. The simulation of varying outlet pressure for the nozzle with 10 inches inlet diameter and 5.75 inches outlet diameter shows that the static pressure difference remains constant to obtain the same velocity. Again, mesh sensitivity analysis performed for the nozzle with 5.75 inches outlet diameter showed that the results between the fine mesh and the coarse mesh varies by 3%.

Furthermore, it also includes the case study for Saint Augustine, where the size and number of bladders required for a closed system to meet energy demand for a small size population have been analyzed. The study suggests that ten bladders of size $390\,m \times 250\,m \times 3\,m$ are required for generating 15 MW power to meet the demand of a small population size of approximately 14,000.

Acknowledgement

I would like to thank School of Engineering, College of Computing, Engineering and Construction (CCEC) of the University of North Florida. I would also like to thank Taylor Engineering Research Institute (TERI) for giving me an opportunity to work on tidal energy. I wish to express my gratitude to my advisor, Dr. Cigdem Akan: her continuous guidance was a milestone in the completion of this research work. I express my genuine thanks to Dr. Don Resio and Dr. John Nuszkowski for all the invaluable assistance and support they have offered me during this research work. In addition, I would also like to express my special regards to all the professors and the students of TERI who supported me and offered help during my Master's courses. I acknowledge the support and great love of my family who kept me going on to achieve my goal.

Table of Contents

Nomenclature

A: Area

A_{basin}: Surface area of the basin

C: Reduction ratio

d: Diameter

g: Gravitational acceleration

H: Height of the bladder

L: Length of the bladder

N_b: Number of bladders

p: Fluid pressure

P_{inlet}: Pressure at the nozzle inlet

Q: Volumetric flow rate

R: Tidal variation

Re: Reynolds number

u: Fluid velocity in the x-direction

v: Fluid velocity in the y-direction

V: Fluid velocity

w: Fluid velocity in the z-direction

W: Width of the bladder

z: Elevation of water

Greek Symbols

ρ: Density of the fluid, kg/m^3

γ: Specific weight of the fluid, kN/ m^3

μ: Dynamic viscosity, kg/ (m.s)

η: Efficiency of the nozzle

Abbreviations

GW: Gigawatt

KE: Kinetic energy

km: Kilometer

KW: Kilowatt

m: Meter

m^2: Square meter

MW: Megawatt

mm: Millimeter

Pa: Pascal

s: Second

List of Figures

List of Tables

1. Introduction

The goal of this research is to optimize the nozzle used in a patented, closed tidal power system that operates effectively in head as low as 0.61 meters. This system exchanges water between two bladders, one onshore and one offshore, to avoid undesirable environmental effects due to exposure of living organisms to moving turbines and to minimize biofouling within the overall power system. Before this new system, only a few sites in the world were suitable for tidal plants since they required at least 5 meters of tidal difference (Etemadi et al., 2011) for economic feasibility. Developing such a renewable Tidal Energy Conversion System (TECS) will increase the number of sites suitable for tidal power plants, and lower operational costs, which eventually will increase the renewable energy potential available throughout the world. The main purpose of this thesis is to optimize the nozzle within this new system to make tidal power generation feasible even in the sites with low tidal range, such as found in many areas along the east coast of the United States. Furthermore, the closed tidal power system that depends on the nozzle for the power generation will eliminate many problems implicit in traditional systems, i.e., tidal barrage, tidal lagoon, and tidal stream. Such a system has the potential to eliminate the primary sources of system biofouling, minimize negative impacts on the local ecology, and provide for efficient and economical deployment and maintenance of the system.

1.1 Context and Motivation

The global demand for energy is rising day by day due to population growth. To meet the energy demand, the world is dependent on fossil fuels, which not only have a limited supply but also harm the environment when burned (Hodges, 2018). The depletion of non-renewable sources on continuous use of it is inevitable (Patel, 2019). Thus, the alternative source of energy has become a subject of concern and need to produce clean energy (i.e., the energy produced without polluting

the environment). In today's context, it is important to focus on renewable sources of energy, e.g., wind energy, solar energy, hydro energy. Ocean energy, further classified into wave energy and tidal energy, is also one type of renewable source among them. In recent years, solar and wind energy has gained popularity, but ocean energy is still lagging.

Approximately 70% of the Earth's surface is covered with water; still, only 16% of energy comes from water resources. While there are several sources of renewable energy, plausibly ocean can be the most relevant source of power generation. This is because waves and tides of the oceans have a massive amount of untapped energy stored. Tides are the result of the gravitational pull of the moon and sun, whereas waves are formed by the wind force exerted on the water surface. Therefore, tides are more predictable than waves.

Extracting energy from tides is an old concept. Despite offering significant potential to use as an alternative source, there are only a limited number of tidal power stations in the world. To meet the energy demand the world is dependent on fossil fuels. Relying on non-renewable sources of energy to meet energy demand cause their depletion along with radiation risks (i.e., emission of energy in the form of electromagnetic waves), acid rain (i.e., precipitation with acidic components as a result of pollution), and emission of gases responsible for global warming (increase in temperature of the Earth). That is why there is a need for clean and renewable energy sources. Unlike tides, solar, wind, wave energy depends on the climate and hence, works better only when the weather is favorable. Therefore, tidal power can be a good alternative as it is incredibly predictable and stable with large potential, and it does not produce air pollution or thermal pollution (degradation of water quality by any process that changes the ambient temperature of water) (Lovejoy, 2018). Even though tidal power is a good alternative for a renewable source of energy, it has some demerits as well. It causes bio-fouling, affects the local ecology, harms the

aquatic life, nutrients important for aquatic life stirs up due to turbulence, 80 % of small fishes passing the turbine are killed, alter currents due to obstruction and so on (Van Haren, 2010).

In a simple term, tidal power is defined as a renewable and predictable source of energy capable of converting energy stored in tides into the electrical energy. Globally, the total energy contained in tides is 3,000 GW (Selin, 2019). There are a few different ways which can capture tidal energy, but the general principle is changing tides run through turbines to generate electricity (Dempsy, 2016). The kinetic energy is harnessed by accelerating the velocity of the contained fluid as it approaches the turbine with the help of the nozzle. The various proposed methods for tidal power generation are tidal stream generators, tidal barrages, and tidal lagoon. According to the US Department of energy, tidal barrage power plants demands at least 16 feet of tidal difference, and globally there are only 40 such sites (Etemadi et al., 2011). Even though tidal barrages are mature and reliable technology for power generation, they have some environmental impacts(Etemadi et al., 2011).

The hypothesis that drove the research on tidal power is the enormous amount of energy stored in tides in the form of kinetic or potential energy that can be converted to electrical energy. The fact that tides are renewable as well as predictable motivated to perform a further study on this topic. Additionally, a few sites in the world are suitable for tidal plants as it requires at least 5 m of tidal difference. This encourages working further on the system that requires tidal lower difference. Plus, the need for renewable sources of energy encouraged studying more about alternative sources focusing predominantly on tidal energy. Lastly, the fact that despite possessing tremendous potential, it is still in its infancy, is the reason to focus on tidal power.

1.2 Objectives

The primary objective of the research is to utilize high-resolution 3-D numerical tools to optimize methods being developed to harness tidal energy. This patented system converts kinetic energy from accelerated flow through an optimized convergent nozzle. This closed system can avoid biofouling (i.e., fouling of pipes as a result of interaction between the membrane materials, fluid flow parameters, and accumulated microorganisms on a wet surface), does not release harmful pollutants into water, and does not affect the marine life or aquatic ecosystem. The specific goals of this research are as follows:

1. To investigate power production by a system that can work under small head differences (e.g., 2 feet), where head difference refers to the difference in the height of high tide and low tide. This will encourage the development of power plants, even in areas with a small tidal difference.
2. To model water flow through a nozzle using 3D design and computational fluid dynamics software, ANSYS.
3. To optimize nozzle efficiency.

This research focuses mainly on the optimization of the nozzle. Still, the optimization of the nozzle requires working on various parameters like the size of the inlet and outlet, angle of the nozzle, exit and inlet ratio, and the relationship of nozzle design/performance as a function of head difference. To achieve the above objectives, first, the outlet and the inlet velocity were calculated using Bernoulli's equation. The calculated inlet velocity was used as the initial boundary condition. Keeping the boundary condition same, flow through the nozzle with various dimensions were simulated using the software, ANSYS. The details are mentioned in the upcoming Chapters 5 and 6.

The results from ANSYS can be used for comparison to experimental results. Performing small-scale tests for various dimensions of the nozzle is not feasible. Optimizing the nozzle using ANSYS saves time; helps to choose the dimensions that look promising for the small-scale and intermediate-scale tests.This makes it possible to study the prototype numerically that can be tested later by experimentation.

1.3 Organization of the Thesis

The organization of the thesis is as follows: Chapter 2 presents a literature review on tidal energy. This section briefly discusses different approaches for power generation, as well as existing tidal power plants. The theoretical background is described in Chapter 3. Chapter 4 presents a case study where energy production potential for the City of St. Augustine is discussed. Chapter 5 presents system optimization. The modeling approached is explained in Chapter 6, followed by a discussion of simulation results in Chapter 7. Finally, Chapter 8 presents the conclusions reached by the current research together with recommendations for future work.

2. Literature Review

Harnessing energy from the tides is not a recently developed technology. Tide mills are evidence that the potential energy stored within the rise and fall of tides is being exploited at a small scale from centuries (Neill et al.,2018). Tidal power was also used for dredging a shipping channel in Hayle, England (Wemyss, 2014). Even though tidal energy came into practice way back, it's still in its early stages. In the 19th century, the world's first tidal power plant named Rance Tidal Power Station was constructed, which has a capacity of 240 MW. Today it's the world's oldest and second biggest tidal power station, which has been operational since 1966 ((EIA), Tidal Power, 2019). During the 20th century, engineers made headway to use tidal movement within the areas with a significant difference in high tide and low tide to generate electricity (Geographic, n.d.). Currently,

few tidal power plants are operating. Sihwa Lake Tidal Power (254 MW), Rance Tidal Power Station (254 MW), Annapolis Royal Generating Station (20 MW) are the largest among operating tidal plants in terms of power output.

2.1 Tidal Energy Generation Methods

The traditional method of harnessing tidal energy utilizes the potential energy conserved in the alternating rise and fall of the sea level. Figure 1 and 2 illustrates the general working principle of tidal plants. During high tides, water flowing from sea to tidal basin hitting the turbine is captured and later released during low tides, which again travels via the turbine to generate power.

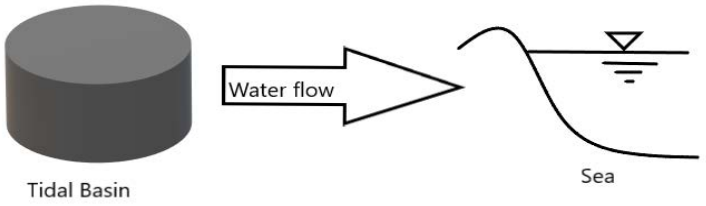

Figure 1: Schematic arrangement of low tide period (Adapted from Vikas Khare, 2018).

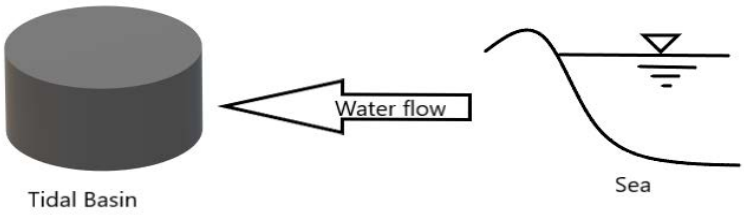

Figure 2: Schematic arrangement of high tide period (Adapted from Vikas Khare, 2018).

The energy stored in tides has both kinetic and potential components. Either of the components can be employed for electricity generation. Some tidal plants use potential energy, whereas some

use kinetic energy. The different methods for harnessing tidal energy are as follows: Tidal barrage, tidal lagoon, and tidal stream.

2.1.1 Tidal Barrage

The Tidal barrage power plant represents a system that makes use of the dam-like structure for storing water and built across a bay or estuary experiencing at least 5 m of tidal difference (Etemadi et al., 2011). There are 23 tidal locations globally, which are technically feasible for tidal barrages, and the mean tidal range at those locations varies from 4.5 m to 12.4 m (Neill et al., 2018). This system uses potential energy to generate electricity. The basic principle of the plant operation is to collect flowing water from the sea to the barrage during high tides and then allowing it to flow from barrage to sea during low tide periods. During both processes, the water turns the turbine and electricity is generated. The power output is proportional to the product of the area of the tidal basin and the square of the head difference (Neill et al., 2018).

$$P = A_{Basin} \times H^2 \quad (1)$$

where P is the power output, A_{Basin} is the area of the tidal basin, and H is the difference in the height of the tide and low tide. Tidal barrages are further divided into the single-basin system and double-basin systems. Single basin system has only one basin while double-basin system has two basins.

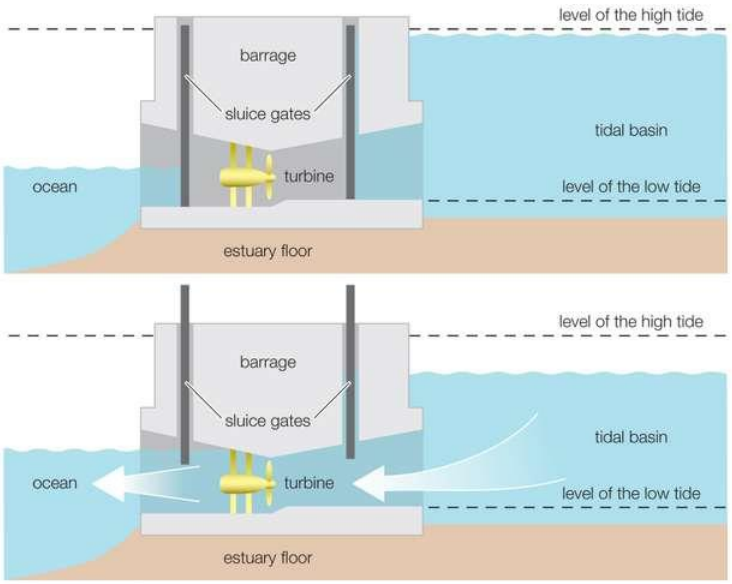

Figure 3: Tidal power barrage (Selin, 2019).

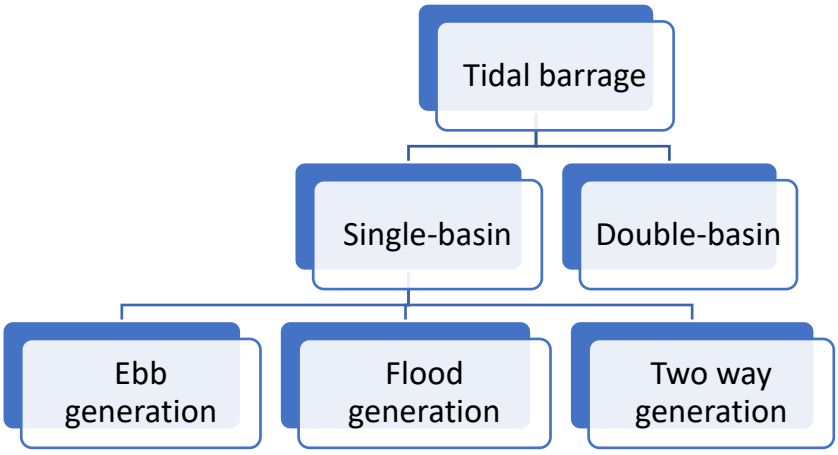

Figure 4: Types of tidal barrage.

2.1.2 Tidal lagoon

A tidal lagoon is the type of tidal power system in which a body of ocean water is partially enclosed by a natural or manmade barrier ((EIA), Tidal Power, 2019). Like barrages, it also uses rising and falling movement of the tide for power generation. The power plant could also generate continuous power ((EIA), Tidal Power, 2019). But this type of power plant is not constructed yet. There are six technically feasible locations for tidal lagoons in the world. (Neill, 2018).

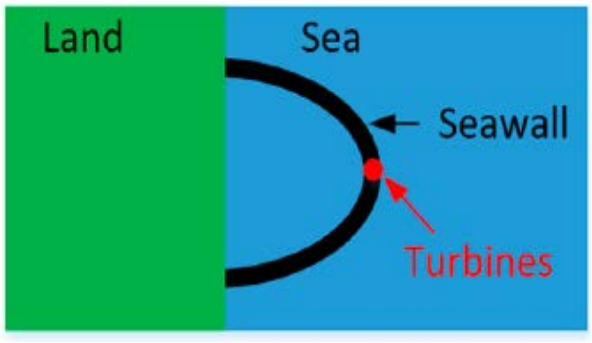

Figure 5: Tidal lagoon (Todeschini, 2017).

2.1.3 Tidal Stream or Tidal Current Turbines

The tidal current turbine works similarly to windmills but, tidal current turbine experiences higher forces and moments than wind turbines (Rourke, 2009). This is because they operate in water. It converts kinetic energy into electricity. Horizontal axis tidal current turbine (the turbine blades rotate parallel to the direction of the flow of water) and vertical axis tidal current turbines (the turbine blades rotate perpendicular to the direction of flow of water) are the methods of extracting energy (Rourke, 2009).

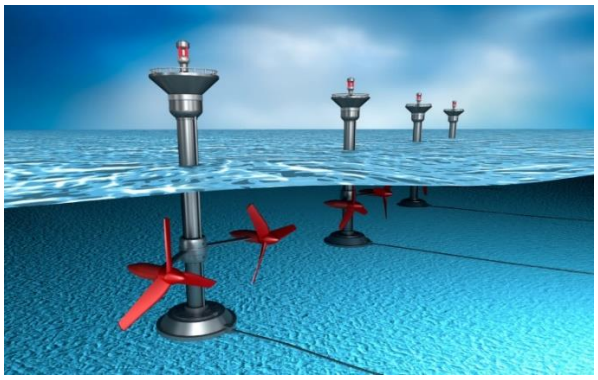

Figure 6: Tidal stream generators (Woo, 2017).

2.2 Description of the System to be Optimized

The working principle is the same as tidal barrages but, instead of using a dam-like structure, bladders are used to store water. The system in this research consists of three main components:

- Bladders: The system comprises two bladders, one onshore and other offshore, as shown in Figure 12. Water flows in either direction through the turbine, depending on the rise and fall of the tide. During low tide, water flows from onshore bladder to offshore bladder via the turbine, as shown in Figure 7. During high tide, the water above the offshore bladder exerts pressure on it, which allows water to flow into the onshore bladder via the turbine, as shown in Figure 7.
- Nozzles: The head above the offshore bladder is two feet, which is not enough to allow fluid to exit the outlet with velocity required to hit the blades of a turbine. Head is the difference in the height of high tide and low tide. So, before hitting the turbine, the velocity of water flowing out through the exit of each bladder is increased with the help of an optimized nozzle.
- Turbine: Turbines are located between two bladders so that when waters travel in both directions (i.e., sea to land or land to sea), it passes via the turbine and generates electricity.

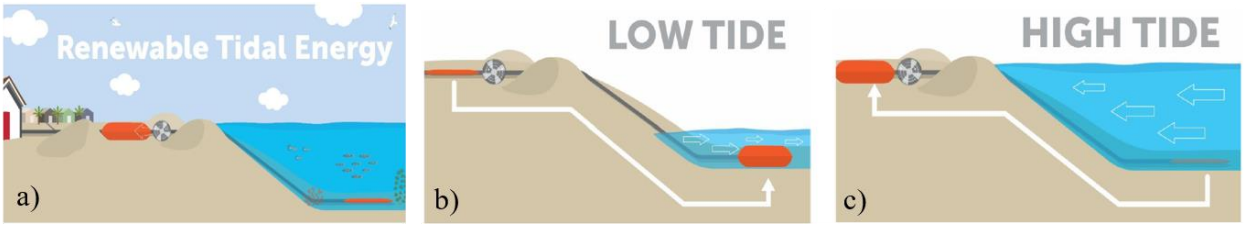

Figure 7: a) Infographic illustrating the proposed closed convergent tidal system; b) Low tide infographic of the proposed tidal system; c) High tide infographic of the proposed tidal system (Vieira, 2018).

2.3 Research into the Estimation of Tidal Power Potential

Various research works have been performed on tidal energy since tides are extremely predictable. There are several research and case studies for the places experiencing a significant tidal difference, and engineers have proposed various tidal power projects. For instance, Swansea Bay Tidal Lagoon was proposed by the United Kingdom, but later it was unapproved by the government. If built, it would have become the world's first tidal lagoon power plant with a capacity of 320 MW using bulb turbines with power enough for 155,000 homes (Waters & Aggidis, 2016).Tidal lagoon designed to convert potential energy into electrical energy sustain less environmental impact (Dixon, 2017).

It is recognized that tides have energy occupy both in kinetic and potential form. That is why both kinetic and potential energy stored in tides can be used to generate electricity. Tidal barrages employ potential energy, whereas tidal streams make use of kinetic energy. The estimate of the energy available for power generation by tidal barrages are between 120 and 400 GW, depending on the location and the potential for conversion (Selin, 2019). The total theoretical available power from the tidal stream in the USA is 50,783 MW (Corporation, 2011).

2.4 Research in Modeling Approaches

Research on tidal energy is not a new thing. Engineers have been researching tidal energy for years. Various approaches can be implemented for modeling tidal power plants. Research on tidal power generation by a closed system is not an entirely new concept. An experiment was conducted by Viera (2018), using small-scale physical model, which allowed testing for the hypothesis that a fluid can be driven against the gravity in a closed system, and the effect of convergent pipes and nozzles for optimizing fluid velocity through the closed system. Furthermore, a numerical model of a system to estimate its behavior and investigate theoretical fluid velocity and associated power

output was created (Viera, 2018). The result from this research revealed that the contained fluid is forced through the nozzle to optimize the fluid velocity.

The objective of the research discussed in this paper is similar to the research explained in the previous paragraph, but it is principally focusing on the optimization of the nozzle. For this research, the nozzle is considered an important component contributing to power generation. This is because the mathematical expression employed in this research depends on two variables, the exit area of the nozzle and exit velocity of the nozzle.

Nozzles are used in various engineering applications wherever there is a need to accelerate or decelerate the fluid flow. There is a good deal of research on nozzle performance as well as on nozzle structures. For instance, one of the canals in Pakistan was exploited for the analysis of flow acceleration by converging nozzle for power generation by run-of-river turbines in open flow channels. Three different cases were analyzed and modeled in fluid dynamic software. The test cases are as follows: a 500 m length of the unpolluted channel, channels with 50 m long nozzles of a different angle (5°, 10°, 20°, and 30°), and channels with 20 nozzles and a water wheel (Khan et al., 2013). The results for the case of the channel with 50 m long nozzles with the different angles revealed that: the increase in velocity for the angle 25° is higher, but other effects are similar, the increase in velocity of water due to presence of the nozzle with an angle less than 20° does not reach the required value for this research (Khan et al., 2013). This result of this research indicates the importance of a nozzle angle. The angle of the nozzle is one of the parameters that need to be optimized.

Furthermore, the investigation of the effects of variation in geometry on incompressible flow in a nozzle by Shademan et al. (2014) was carried out. The nozzle used in the hydraulics laboratory at the University of Windsor for submerged jet research was considered as the baseline nozzle, which

is 70 mm long, 50 mm in diameter at the inlet, and 10 mm diameter at the outlet (Shademan et al., 2014). Three additional nozzles with slight modification from the baseline nozzle were modeled to investigate the effect of nozzle configuration on the turbulence characteristics of the flow of water through nozzles. The results from this investigation revealed that even a small change in the nozzle could result in major changes to the operating conditions of the nozzle.

In addition, in 2013, flow behavior in various nozzle shapes in hydroentangling nozzles was modeled by Poudeyhimi and Tafreshi. They considered two sets of nozzles to study the effect of cone angle and nozzle aspect ratio (the ratio of its capillary section to its diameter). The first set consists of an aspect ratio of 1 and varying cone angles of 19, 15, 11, 7, and 3° respectively while, the second set consists of varying aspect ratio (1 to 6) and fixed inlet and outlet diameters (Pourdeyhimi & Tafreshi, 2013). The results revealed that a decrease in cone angle or increase in the aspect ratio did not affect hydroentangling waterjet nozzles.

Budiyanto et al. (2019) performed the analysis of the nozzle by comparing the working of the convergent and convergent-divergent nozzle of waterjet propulsion that uses momentum change as the working principle. Waterjet propulsion is utilized by ship for high-speed operation and sailing in shallow waters. The nozzle with an inlet diameter of 77 mm and varying exit diameters were analyzed in ANSYS FLUENT. For boundary conditions, initial velocity and gauge pressure were 6 m/s and 30,000 Pa, respectively. The results from the analysis revealed that the convergent nozzle is desirable for saving energy in waterjet propulsion as its efficiency is higher than the combination nozzle (Budiyanto et al., 2019).

3. Theoretical Background

This chapter provides a short overview of basic concepts on tides and tidal forces.

3.1 Basic Concepts

Tides are the result of the gravitational pull of the moon, whereas waves are formed by the winds. Because tides are formed by the gravitational attraction of the sun and moon, they are outstandlingly predictable. The alternating rise and fall of the sea level are outlined as a tide. In fact, tides are exponentially long-period waves that start within the ocean and move towards the coastline, where they appear as alternating rise and fall of the sea level (Patel, 2019).

In 1687, Newton illustrated that the gravitational attraction of the sun and moon on the earth tides are responsible for the formation of ocean tides (NOAA, n.d.). The tidal force, which causes the Earth and its water to bulge out on the sides closest and farthest from the moon, is the result of the gravitational pull of the moon (SciJinks, 2019). When the gravitational pull of the sun and moon are fused, more extreme high and low tides occur. High and low tides happen about every two weeks when the Earth, the moon, and sun line up, which happens at times of the full moon or new moon (SciJinks, 2019).

There are three basic types of tides: semidiurnal, mixed, and diurnal (NOAA, 2000). The semidiurnal has two high tides of almost equal height and two low tides of almost equal heights each tidal day. The time of rotation of the Earth with respect to the moon is known as tidal day, mean value is approximately equal to 24.84 hours (NOAA, 2000). The mixed tide is different from semidiurnal in that the two high waters and the two low waters of each tidal day have marked differences in their heights. In some places, tides cause water levels near the shore to vary up to 40 feet ((EIA), Tidal Power, 2019).

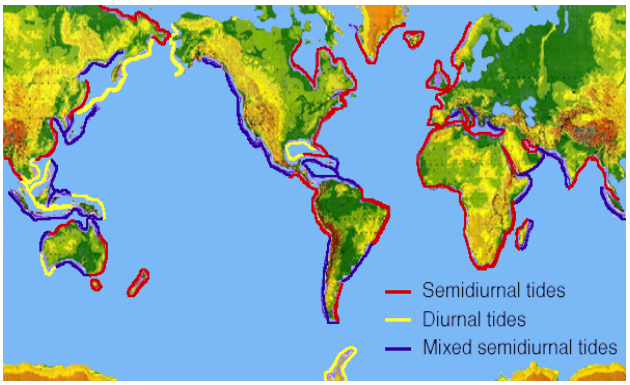

Figure 8: Map showing the geographic distribution of different tidal cycles. (NOAA, n.d.).

In Figure 8, red color represents the coastal areas experiencing semidiurnal tides, yellow color represents areas experiencing diurnal tides, and blue color represents the area with mixed semidiurnal tides.

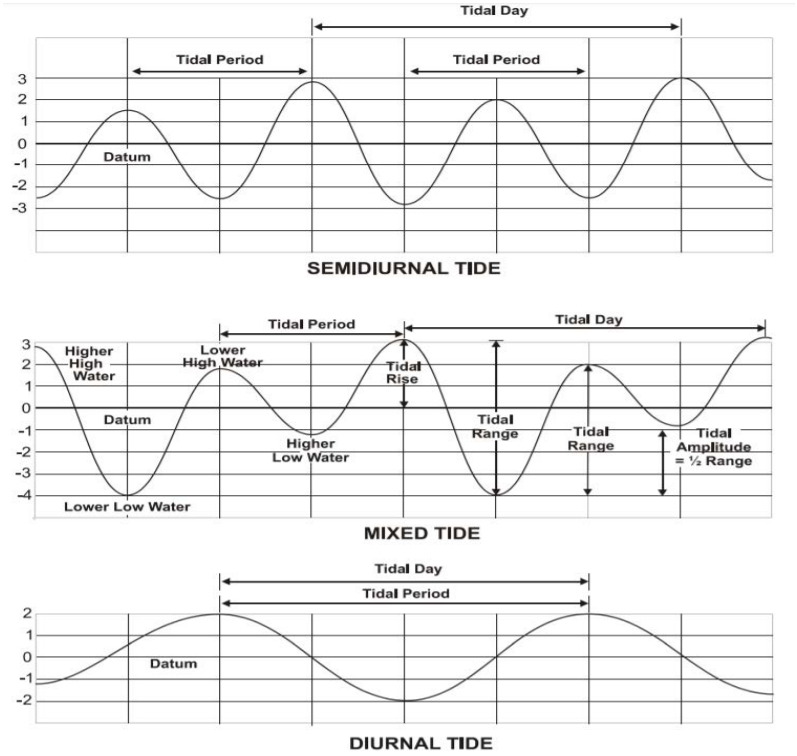

Figure 9: A depiction of the three primary kinds of tides. The zero on these graphs is illustrative of the relationship of the tides to Mean Sea Level (MSL) (NOAA, 2001).

The gravitational attraction produced by the moon and sun reinforces each other at times of new and full moon to heighten the range of the tides and counteract each other in the first and third quarters to reduce the tidal range. Spring tides are the largest tide that is produced at the new and full moon. The smallest tides, neap tides, occur during the first and third quarters of the moon (NOAA, 2001).

3.2 Tidal Forcing

Tidal force can be defined as the contrast between the gravitational force at the center and the locations away from the center, and these forces would diminish to zero at the center (Samuel J. Ling, 2020). An object is in a stable free-fall orbit if the gravitational force acting on it is balanced with the centrifugal force of its motion. Even though the center of mass of the Earth is in free-fall orbit, the locations away from the center experience a slight difference in gravitational force and the centrifugal force of the orbital motion, and there is a small residual force which is known as tidal force (Cramer, 1994).

3.3 Governing Equations

Like all other fluid flow problems, the fundamental governing equations are the set of Naiver-Stokes equations for an incompressible, constant viscosity fluid.

$$\rho\left(\frac{\partial u}{\partial t}+u\frac{\partial u}{\partial x}+v\frac{\partial u}{\partial y}+w\frac{\partial w}{\partial z}\right)=\mu\left(\frac{\partial^2 u}{\partial x^2}+\frac{\partial^2 u}{\partial y^2}+\frac{\partial^2 u}{\partial w^2}\right)-\frac{\partial p}{\partial x}+\rho g_x \quad (2)$$

$$\rho\left(\frac{\partial v}{\partial t}+u\frac{\partial v}{\partial x}+v\frac{\partial v}{\partial y}+w\frac{\partial v}{\partial z}\right)=\mu\left(\frac{\partial^2 v}{\partial x^2}+\frac{\partial^2 v}{\partial y^2}+\frac{\partial^2 v}{\partial w^2}\right)-\frac{\partial p}{\partial y}+\rho g_y \quad (3)$$

$$\rho\left(\frac{\partial w}{\partial t}+u\frac{\partial w}{\partial x}+v\frac{\partial w}{\partial y}+w\frac{\partial w}{\partial z}\right)=\mu\left(\frac{\partial^2 w}{\partial x^2}+\frac{\partial^2 w}{\partial y^2}+\frac{\partial^2 w}{\partial w^2}\right)-\frac{\partial p}{\partial z}+\rho g_z \quad (4)$$

where, μ is the viscosity, u, v, and w are velocities in x-, y-, and z-directions, respectively. Moreover, the conservation of mass in fluid flow is described by the differential continuity equation for an incompressible fluid as:

$$\frac{\partial u}{\partial x}+\frac{\partial v}{\partial y}+\frac{\partial w}{\partial z}=0 \tag{5}$$

Equations (2)-(4), together with the above continuity equation and the relevant boundary conditions, describe the motion of the viscous incompressible fluid flow.

Assuming a steady flow of incompressible fluid without shearing stress, the Bernoulli equation is used to find a velocity through a pipe:

$$\frac{1}{2}\rho\boldsymbol{u}^2+p+\rho gz=\text{Constant} \tag{6}$$

where p is the pressure, $\boldsymbol{u}$ is the 3D velocity field of a fluid, g is the acceleration due to gravity, z is the elevation of water from the datum.

Bernoulli equation state that pressure, potential energy, and kinetic energy per unit volume will remain constant along a streamline.

The kinetic energy is converted into electrical energy in the proposed system. The available power is given by

$$P_{available}=\frac{1}{2}\dot{m}\,V^2 \tag{7}$$

where $\dot{m}$ is the mass flux given as $\dot{m}=\rho VA$. Thus, Eqn. (7) becomes

$$P_{available}=\frac{1}{2}\rho AVV^2=\frac{1}{2}\rho AV^3 \tag{8}$$

where ρ is the density of water, A is the area of a turbine, V is the velocity of a turbine.

4. Case Study: St Augustine, FL

Although Florida offers the potential to generate clean energy, it frequently depends on fossils and lightly on renewable sources. The cities like Saint Augustine, FL, often experience tidal flooding which cannot be avoided but can be utilized for power generation. Tidal power plants are extremely costly, and there are very few tidal plants throughout the world. To demonstrate the relation between the size of the bladder and the power and to determine the power requirement for the scanty population (approximately 14,000), Saint Augustine, FL, has been selected for a case study. Saint Augustine is a city in the Southeastern United States, on the Atlantic coast of northeastern Florida, located at 29°53′41″N 81°18′52″W. The area of Saint Augustine is 33.06 km^2, with 24.43 km^2 land and 8.63 km^2 of water. It has a population of approximately 14,000. It encompasses sites with approximately 1.5 to 5 m tidal range. The current state of the art requires a tidal range of at least 7 m for economical operation. But the hypothesis for this research is the power generation under two feet head by optimizing the nozzle within a closed system. The general idea is to determine how much power will be required for each household and what size of the bladder will be required to generate that power.

Next, design considerations for the power required for the houses of Saint Augustine are discussed. Average US home uses 900 kWh per month, which is equal to approximately 30 kWh per day and 1.25 KW per hour. Therefore, the power required per hour per home in a city like St. Augustine, FL, is approximately 1.25 KW. Assuming there are approximately 5,562 houses in St. Augustine, the total power required per hour becomes 7.1 MW.

Next, the minimum required length of the bladder (L) is calculated by keeping width (W), height (H), and the number of bladders (N_b) constant. For the initial design, the following values are used: W = 250 m; H = 3 m, N_b = 10. The velocity of the nozzle is assumed to be varied from 10 m/s to

20 m/s. Note that these initial values are chosen at random. Thus, for $V = 10$ m/s, the length of the bladder can be calculated by rearranging Eqn. (8) as follows:

$$A_{nozzle} = \frac{2 \times P}{\rho V_{nozzle}^3} = \frac{7.1 \times 10^6}{(1000)(10)^3} = 14.2 \text{ m}^2 \quad (10)$$

where ρ is water density taken as 1000 kg/m^3. Volume per unit time is calculated using the relationship $Q = A_{nozzle} \times V_{nozzle}$. Now, the volume of the bladder can be calculated using the relationship $Q = \frac{\text{Volume}}{\text{time}}$ where time is in seconds. It takes approximately 6 hours for the water at the shore to go from high tide to low tide and vice versa.

$$\text{Volume} = 14.2 \times 10 \times 6 \times 3600 = 3{,}067{,}200 \ m^3$$

This is the total volume of the whole system. Again, the volume required of each bladder is obtained by dividing total volume in a system by number of bladders, i.e., $\text{Volume}_{\text{each}} = 306{,}720$ m^3. Using the relationship $\text{Volume} = L \times W \times H$, one can obtain a required length for each bladder as follows:

$$L_{each} = \frac{\text{Volume}_{\text{each}}}{WH} \quad (11)$$

Solving Equation 11, the length of each bladder obtained is 408 m.

For generating 7.1 MW power, one needs ten bladders of dimension $408\ m \times 250\ m \times 3\ m$. Similar calculations were carried out in the MATLAB for the velocities varying from 10 m/s to 20 m/s and for the power out of 7.1 MW, 10 MW, and 15 MW. The velocity used in the calculation is the velocity of the nozzle at the exit.

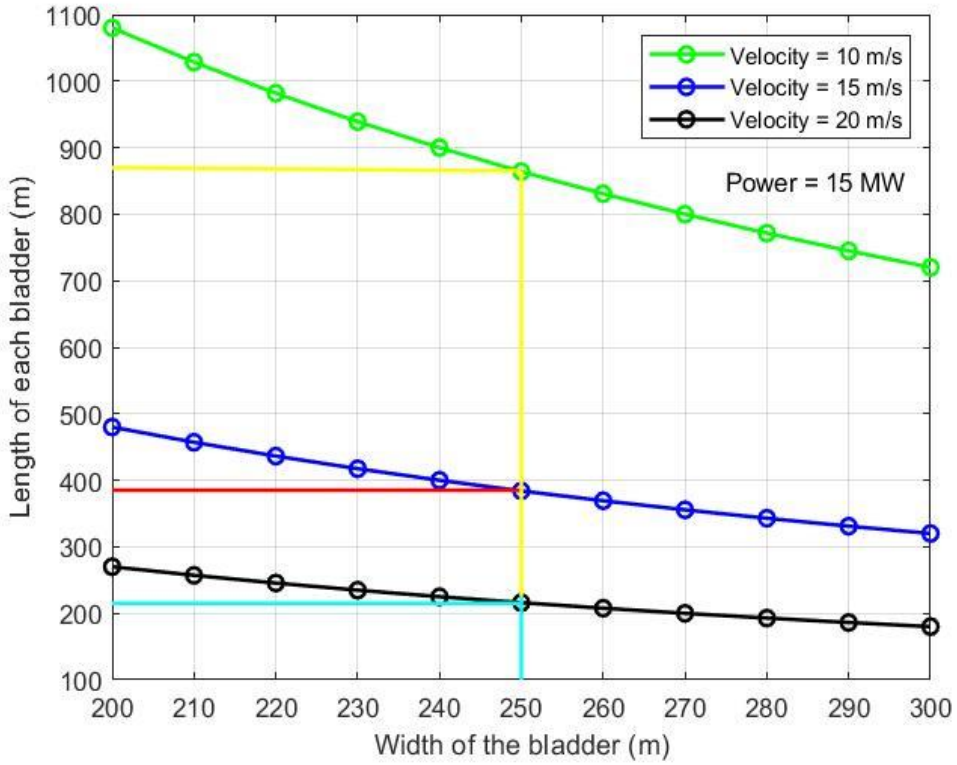

Figure 10: Length of each bladder for varying widths.

The graph representing the relation between the length of each bladder and the width of the bladder when 15 MW power and the velocity of the nozzle is 10 m/s, 15 m/s and 20 m/s is shown in Figure 10. As can be seen from Figure 10, the length of each bladder is decreasing with increasing velocity and decreasing width of the bladder. Recall that, $W = 250$ m is used for the current calculations. When the velocity of the nozzle is 10 m/s, the length of each bladder varies from 1090 m to 710 m approximately. The length of the bladder when the velocity of the nozzle is 15 m/s is almost half of the length of each bladder when the velocity is 10m/s.

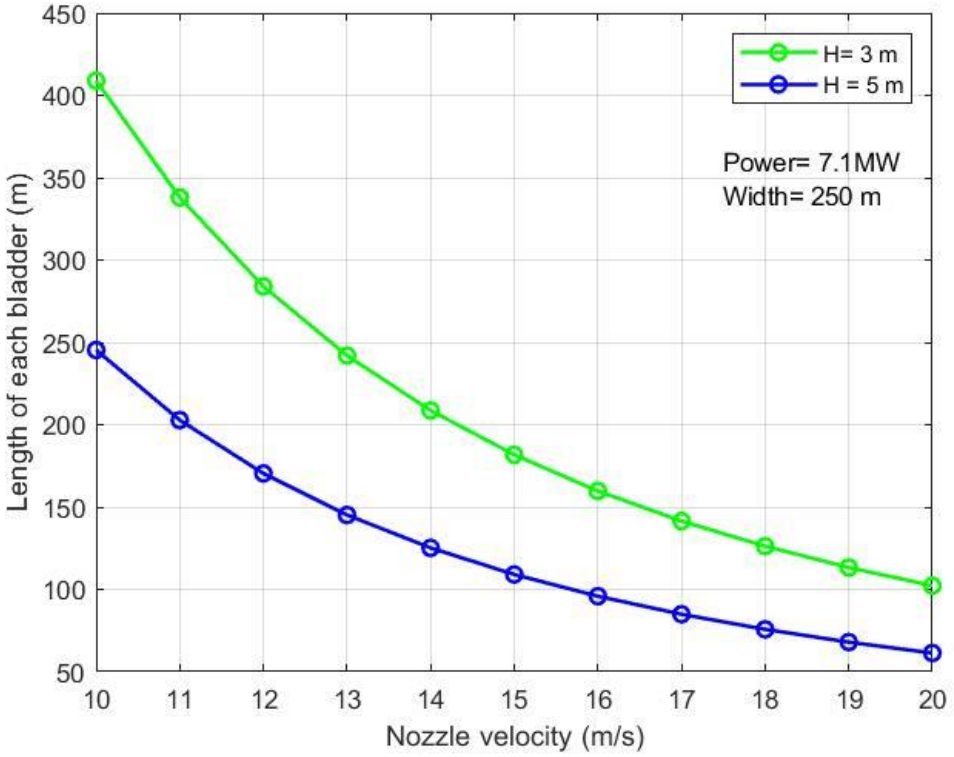

Figure 11: Length of each bladder for varying velocity

Figure 11 represents the length of each bladder for different velocities. The length of the bladder decreases with an increase in the nozzle velocity. One can see from Eqn. 11 that the length of the bladder is inversely proportional to the height of the bladder. Keeping the volume and width constant, the length of the bladder increases with a decrease in the velocity.

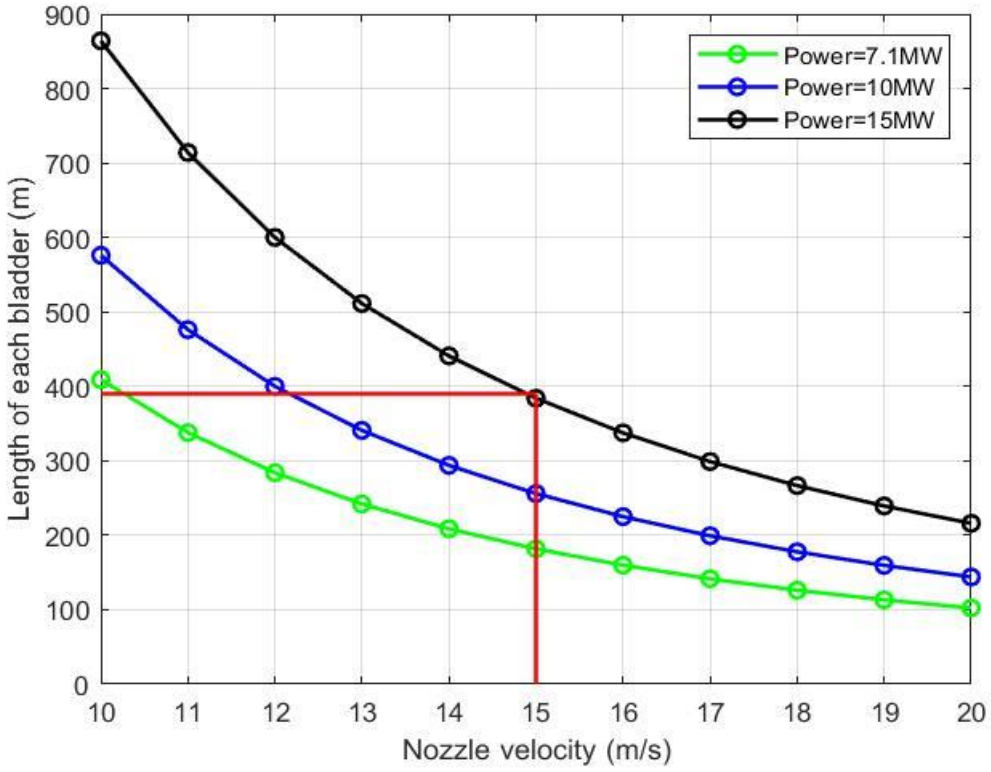

Figure 12: Length of each bladder for varying velocity and power

Figure 12 represents the relation of the length of the bladder for varying power and velocity. For 15 megawatt power, the length of the bladder is approximately 870 m at 10 m/s velocity, which is large. Minimizing the length of the bladder requires an increase in the nozzle velocity. From the above graph, for 15 MW power, the length of the bladder is approximately 950 m, which is close to 1 km when the velocity of the nozzle is 10m/s. If the velocity is increased from 10 m/s to 15 m/s, the length of each bladder becomes almost 2.4 times the length of each bladder when the velocity of the nozzle is 10 m/s. Therefore, the length of the bladder, i.e., approximately 390 m at the velocity of 15 m/s, looks fair. This suggests that ten bladders of size $390\ m\ \times 250\ m\ \times 3\ m$ are required to generate 15 MW power.

Furthermore, the power out given by the closed system is compared with the power given by the mathematical expression derived in the research paper by Tausif Ali et al. (2012). The potentiality of tidal power in Swandwip, an island along the southeastern coast of Bangladesh, was analyzed using the mathematical regime that is associated with two variables, surface area of the basin and tidal variation. The expression is given by:

$$P_{actual(one\ way)} = 0.028\ A_{basin} R^2 \quad (12)$$

$$P_{actual(two\ way)} = 0.056\ A_{basin} R^2 \quad (13)$$

Where, A_{basin} is the surface area of the basin, and R is tidal variation.

Keeping the area of the tidal basin same as the area of the bladder, the power output for both systems was calculated and compared. The area of the bladder is given by multiplying the length and width of the bladder, i.e., 306,720 m^2. The area of the basin is the same as the area of the bladder. Using Eqns. 12 and 13, power outputs are calculated as 5.3 KW and 10.7 KW for one way and two-way technology, respectively. A closed system using a nozzle gives larger output in comparison to the barrage system for the same head and the area for storing water. This is because the traditional method (i.e., the barrage system) is proportional to the square of the tidal variation, while the closed system described in this paper is proportional to the square of the exit velocity of the nozzle.

5. System Optimization

This section presents a sample calculation for optimizing the exit area of a nozzle. First, the sample for calculating the exit area required for a nozzle to maintain the velocity approximately 10 m/s is illustrated. For this purpose, Bernoulli and continuity equations are used. The arrow in Figure 13 shows the direction of flow.

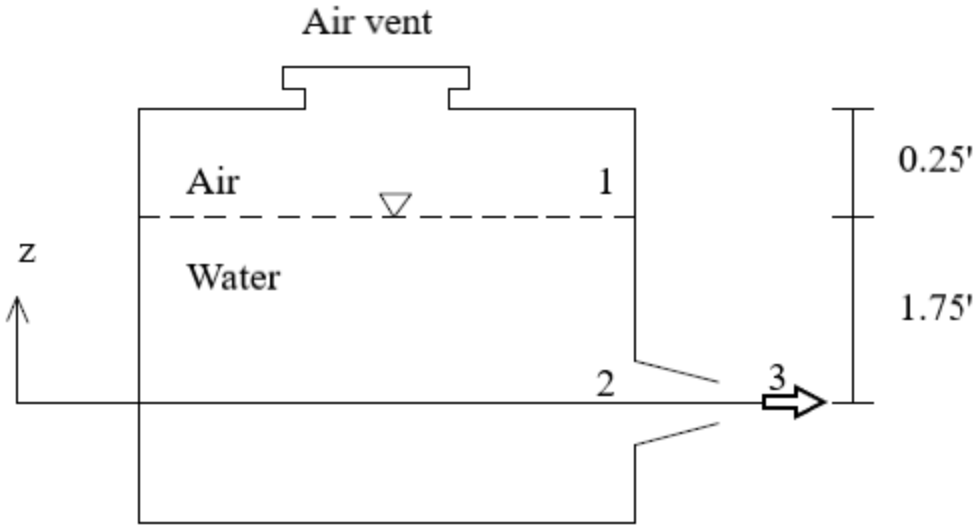

Figure 13: Open tank with a nozzle

With the vent open:

For steady, inviscid, incompressible flow, the Bernoulli equation applied between points (1) and (3) gives

$$\frac{p_1}{\rho} + \frac{1}{2}V_1^2 + gz_1 = \frac{p_3}{\rho} + \frac{1}{2}V_3^2 + gz_3 \quad (14)$$

With the assumptions that $p_1 = p_3 = 0$, $V_1 \approx 0$, and $z_3 = 0$, Eqn. 14 becomes

$$\rho g z_1 = \frac{1}{2}\rho V_3^2 \quad (15)$$

$$V_3 = \sqrt{2gz_1} \tag{16}$$

Eqn. (16) gives the velocity at the exit of a tank.

$V_3 = \sqrt{(2)(9.81)(0.5334)} = 3.24$ m/s

To maintain the exit velocity at least three times of inlet velocity (recall that we want to have an outlet velocity of 10 m/s), the vent needs to be closed ($P_1 \neq 0$). Then, Bernoulli's equation between points 1 and 3 gives,

$$\frac{p_1}{\rho} + gz_1 = \frac{1}{2}V_3^2 \tag{17}$$

For $V_3 = 3 \times 3.24 = 9.72$ m/s, $p_1 = 41{,}255$ Pa

The exit area of the nozzle (A_3) is calculated by keeping the inlet area of the nozzle (A_2) and the velocity at nozzle inlet (V_2) constant. For the initial design, the following values are used: diameter of the inlet, d_2 = 0.254 m (10 inches), V_2 = 3.24 m/s, d_3 = 0.146 m (5.75 inches)V_3 = 9.72 m/s

Applying the continuity equation shown in Sections 2 and 3,

$$A_2V_2 = A_3V_3 \tag{18}$$

Exit velocity of the nozzle is calculated by rearranging the Eqn. 18

$$V_2 = \frac{A_3V_3}{A_2} = 3.21 \text{ m/s} \tag{19}$$

The calculated inlet velocity is used as a boundary condition for the computational fluid dynamics software, ANSYS FLUENT, which will be discussed in the next section in detail. The numerical simulation of fluid flow of the nozzle with inlet diameter 10 inches and outlet diameter 5.75 inches is performed to compare the values obtained in the above calculation. The method used for the

simulation is discussed in the upcoming Chapter 6. The boundary condition used for this is as follows:

Pressure inlet: 41,255 Pascal

Pressure outlet: 0 pascal

6. Modeling Approach

This section briefly describes the multiphase flow and volume of fluid methods. Also, it introduces ANSYS briefly as it is used for flow simulation in the nozzle.

6.1 ANSYS

ANSYS, which stands for the Analysis System is an engineering software that uses finite element analysis for simulation of computer models. Finite Element Analysis is the simulation of a physical phenomenon using the Finite Element Method (FEM). FEM is a mathematical technique where a system is subdivided into smaller parts for solving an engineering problem. ANSYS helps to minimize the physical prototype and allows the virtual experiment to optimize the designs. It also helps to design and optimize fluid-related equipment and provides fluid dynamics solution for modeling fluid flow. ANSYS has two solvers, CFX and FLUENT, integrated within the ANSYS workbench framework, numerically solve the fluid flow equations in the computational domain. For this thesis, ANSYS FLUENT has been used.

6.2 Methodology

ANSYS-FLUENT is used for the simulation of fluid flow through various dimensions of nozzles. The modeling of a nozzle in ANSYS-FLUENT involves the following steps:

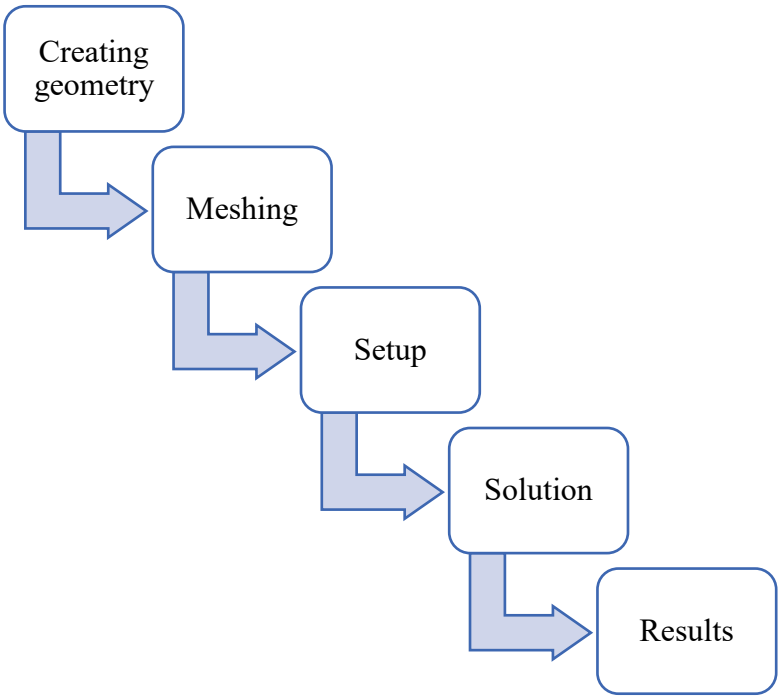

Figure 14: Flow chart for the simulation of fluid flow through a nozzle.

First, the 3-D geometry of a nozzle was created in the design modeler of ANSYS fluent. All the units were set to millimeters before creating the geometry. The dimensions used are shown in the table below:

Table 1: Dimensions of the nozzle.

Inlet Diameter	**Outlet Diameter**
10 inches (254 mm)	7.5 inches (190.5 mm)
	6 inches (152.4 mm)
	5.75 inches (146 mm)
	5 inches (127 mm)
	4 inches (101.6 mm)

Second, geometry was imported to meshing, where the nozzle was meshed, as shown in Figure 15. The element size of 0.002 m was used for meshing. For mesh sensitivity analysis the meshing size was varried from 0.01m to 0.001 m. The sensitivity of the results to mesh sizing is given in Appendix 3. Different sections of the nozzle are named. The entrance of the nozzle is named as inlet, the exit of the nozzle is named as an outlet, and the remaining portions are named as walls.

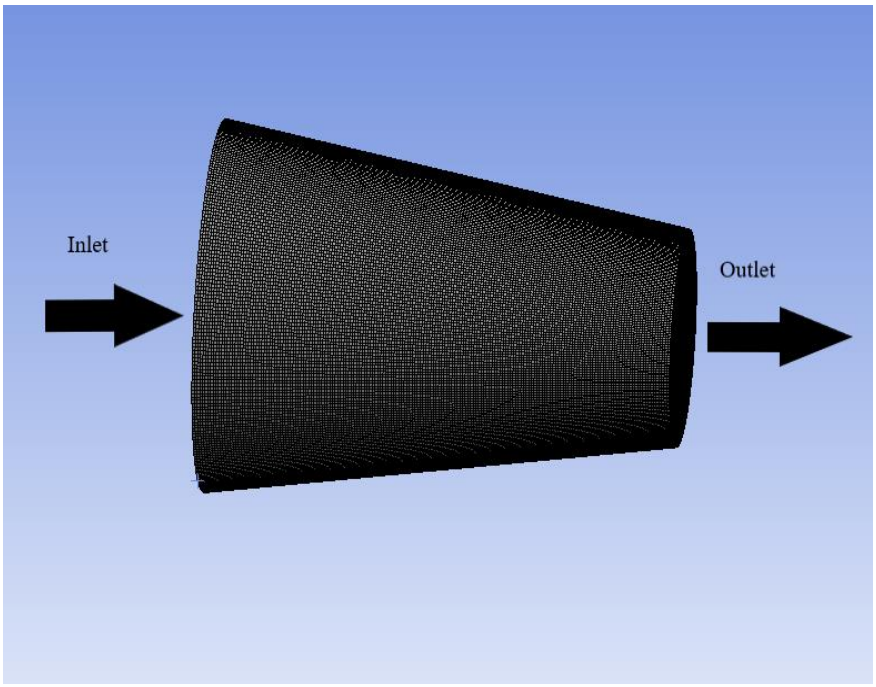

Figure 15: Representation of mesh of a convergent nozzle.

After meshing, the next step is set up, where the required material is added; the model is selected, boundary conditions are defined. For boundary conditions, the velocity at the inlet is 3.21 m/s, which was obtained from the calculation in Chapter 5, and the pressure outlet is 35,000 Pascal. The summary of a setup part is represented in the Table 2. The working fluid is water. After setup, the solution part runs. The last part is the result where simulation is analyzed and represented in a useful form, e.g., contour, streamlines, velocity vectors, volume rendering and so on.

Table 2: Representation of the analysis procedure followed in the ANSYS.

Description	Setup Details
General values	Solver type: Density type Velocity formulation: Absolute Time: TransientS
Model	Viscous (Turbulent) Energy: On
Materials	Fluid: Water-liquid
Cell-zone conditions	Part-water zone: Water-liquid
Boundary conditions	Inlet: Velocity Temperature: 300K Outlet: Pressure
Initialization	Type: Standard Compute from: Inlet
Calculation	Number of time steps: 100

A similar process is repeated for different outlet sizes of the nozzle, and the results are compared with each other. First, the above dimensions were used for simulation in ANSYS-FLUENT. With the same boundary conditions but different outlet diameter, efficiency, and reduction ratio are calculated using the formula (Budiyanto et al.,2019):

$$\eta = \frac{\frac{1}{2}\times\rho\times v^2}{P_i} \tag{20}$$

where, η is nozzle efficiency, ρ is the density of water, v is the jet velocity, and P_i is the water inlet pressure.

$$C = \frac{D_{outlet}}{Dinlet} \tag{21}$$

where, C is reduction ratio, D_{outlet} is the diameter of the nozzle exit, and D_{inlet} is the diameter of nozzle inlet. The motive of calculating the reduction ratio is to observe the ratio of the inlet and the outlet diameter that sets out acceptable efficiency.

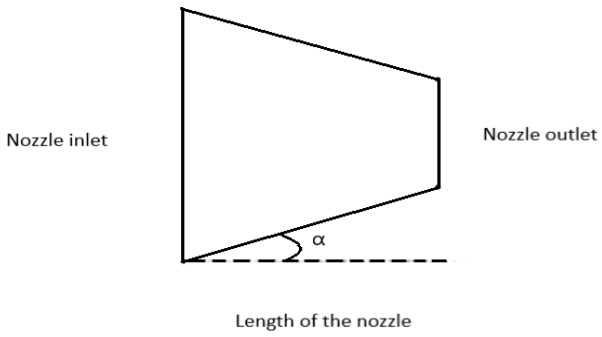

Figure 16: Nozzle showing angle α.

The calculation of efficiency and reduction ratio for different dimensions of the nozzle are listed below in Table 3. The pressure at the inlet of the nozzle is different for different outlet diameter.

Table 3: Calculation of efficiency of the nozzle.

INPUT				OUTPUT			
Inlet diameter (inches)	**Outlet diameter (inches)**	$C = \frac{D_{outlet}}{D_{inlet}}$	**α**	**Outlet velocity (m/s)**	**Inlet pressure (Pascal) (ANSYS)**	**Efficiency (%)**	**Inlet pressure (calculated)**
10	7.5	0.75	5.9	5.87	47,450	36.3	47,092
	6	0.6	9.5	9.1	750,70	54.8	70,984
	5.75	0.575	10	9.8	82,090	58.5	77,871
	5	0.5	11.8	13.34	119,100	74.7	118,830
	4	0.4	14	20.6	243,300	87.2	242,032
	3	0.3	16.3	36.5	690,700	96.4	695,977

Table 3 shows that the efficiency for the reduction ratio 0.6 is 54.5% while, efficiency for the reduction ratio 0.3 is 96.4%. As stated by the Eqn. 20, the efficiency is dependent on the outlet velocity and the inlet pressure. As a consequence, the efficiency is increasing with an increase in the velocity of the nozzle outlet. Tha last column of the Table 3 represents the pressure at the inlet of the nozzle, calculated using the Bernoulli's equation.

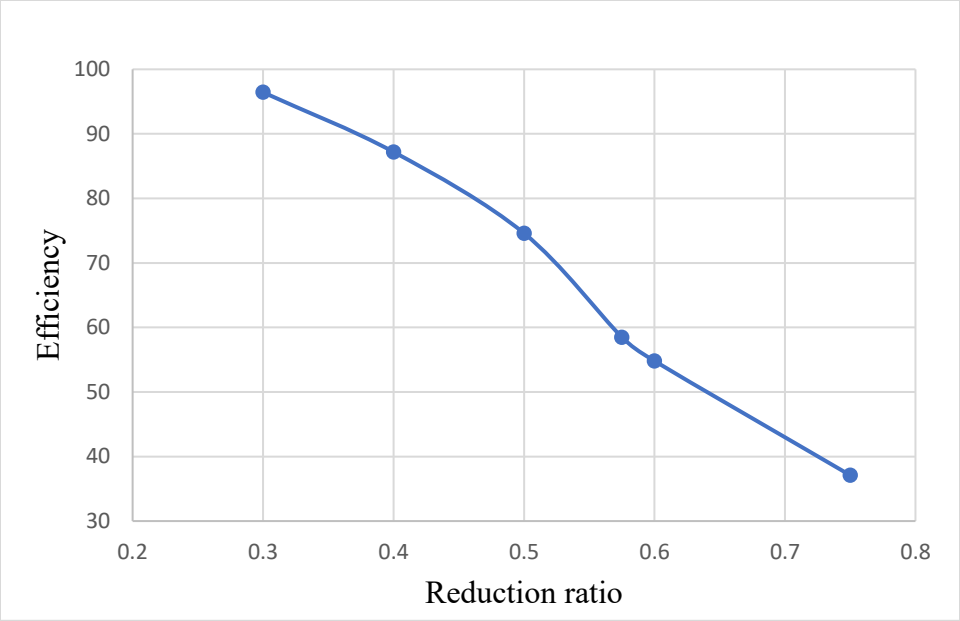

Figure 16: The reduction ratio vs. the efficiency of the nozzle.

From Fig. 16, one can see that the efficiency of the nozzle increases with the increase in the reduction ratio. This indicates that the efficiency of the nozzle raises with the decreasing diameter of the nozzle outlet.

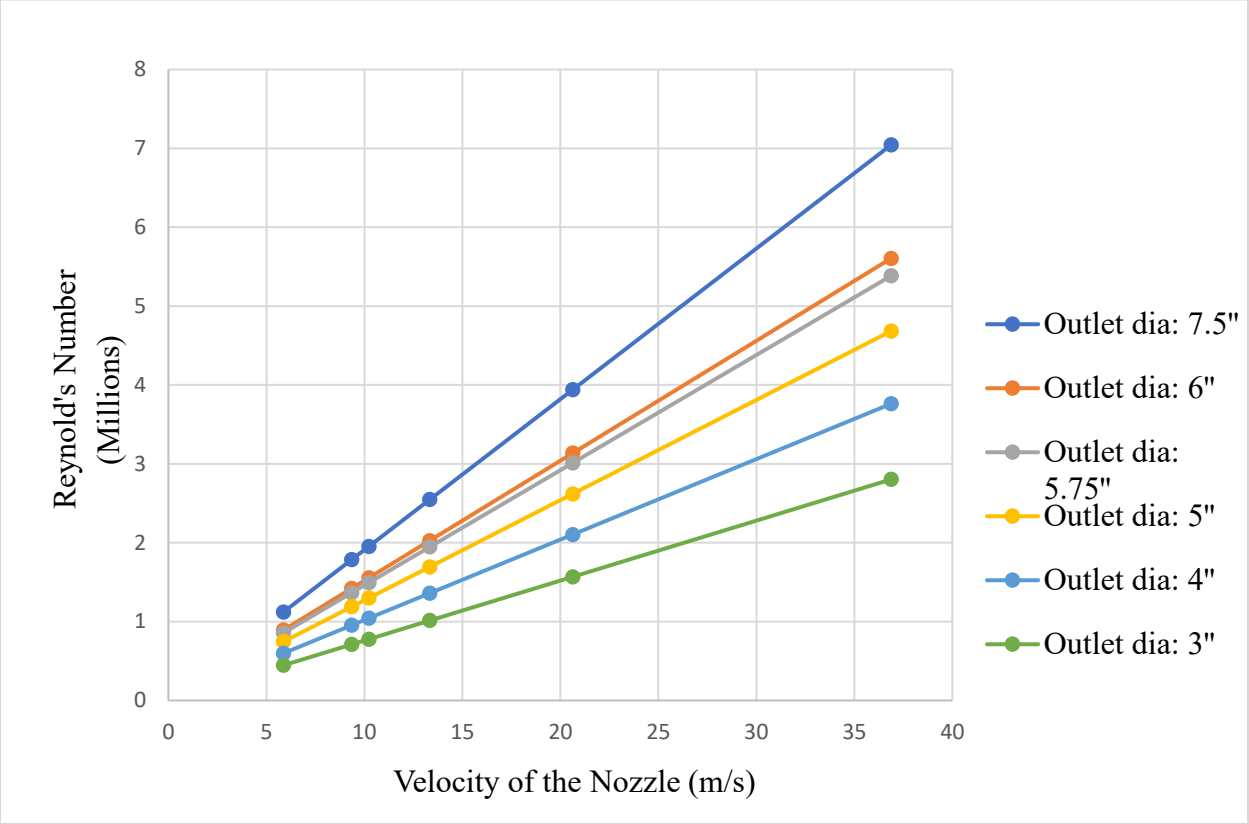

Figure 17: Reynolds Number at the outlet of the nozzle

The Reynolds number shown in Figure 17 suggests that the flow through the nozzle is turbulent as Reynolds number is greater than 4000. The Reynolds number is given by,

$$Re = \frac{V \times D}{\nu} \qquad (22)$$

where Re is Reynolds number, V is the velocity of the fluid flowing through the outlet of the nozzle, D is the outlet diameter and ν is the kinematic viscosity.

The flow is laminar when $Re < 2300$

The flow is transient when $2300 < Re < 4000$

The flow is turbulent when $Re > 4000$

The numerical simulation of the nozzle is again carried out, keeping the boundary conditions the same but changing the model. The results are shown in Appendix 4.

7. Simulation Results & Discussion

This section contains the simulation results run in ANSYS for the nozzle with different sizes.

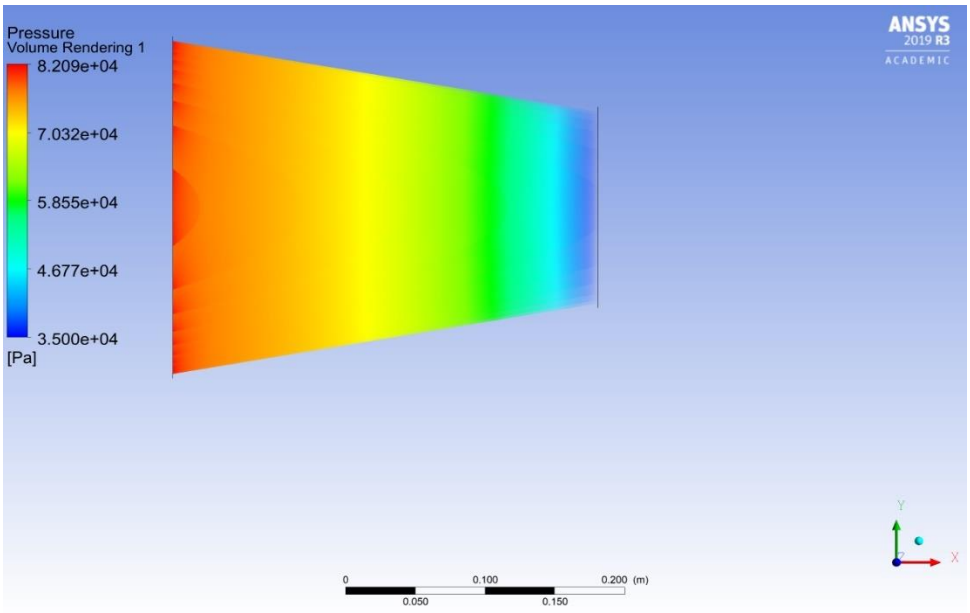

Figure 18: Representation of pressure of the nozzle with 5.75 inches outlet diameter.

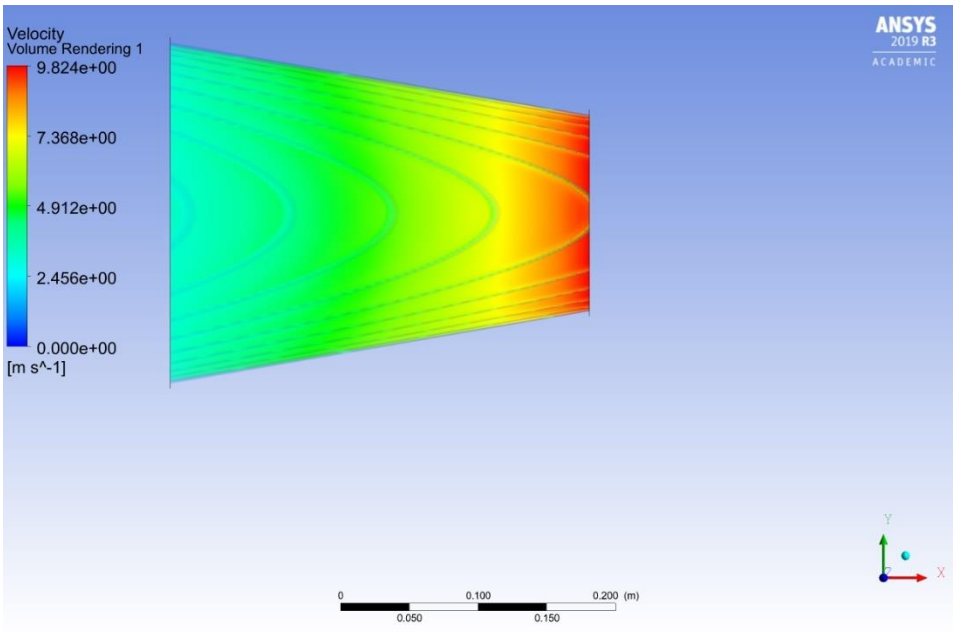

Figure 19: Representation of velocity through the nozzle of outlet diameter 5.75 inches.

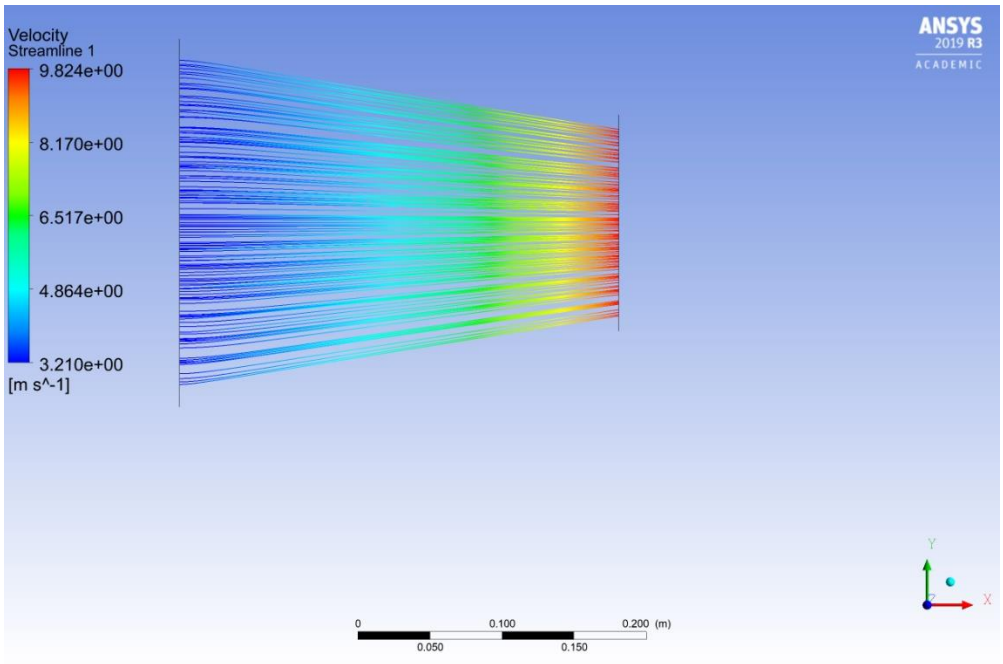

Figure 20: Velocity Streamline of the nozzle with outlet diameter 5.75 inches

The pressure and the velocity volume rendering for the nozzles with outlet diameters 5.75 inches are shown in Figures 18 and 19, respectively. The outlet velocity and inlet pressure of the nozzle

with outlet diameter 5.75 inches are 9.8 m/s and 82,090 Pa, respectively. The inlet pressure is decreasing with an increase in the outlet diameter, i.e., the efficiency of the nozzle also decreases. The efficiency of the nozzle is based on inlet pressure and the outlet velocity. The flow pattern shown in the velocity streamline in the Figure 20 seems to have similar pattern of flow in the velocity streamline of convergent nozzle discussed in the study by Budiyanto et al. (2019). This indicates that the setting of ANSYS Fluent resembles the setting used in that paper. The efficiencies of the nozzle shown in the Table 3 are calculated following the study carried out by Budiyanto et al. (2019) for convergent and convergent-divergent nozzle. Figure 16 shows the efficiency in comparison to the reduction ratio. It suggests that the efficiency of the nozzle increase with the decrease in the reduction ratio. The results are similar to what Budiyanto et al. (2019) reported in their study.

8. Conclusions and Future Work

Tides possess vast energy stored in both kinetic and potential forms. Due to its extraordinarily predictable nature, it demonstrates the ability to play a relevant part in the renewable energy future. There are several methods to employ energy retained in the tides for power generation. Either potential energy or kinetic energy can be utilized. This paper focuses on converting kinetic energy for generating power with the help of the optimized nozzle. All the calculations and the simulation are performed, assuming the static pressure. This implies that the head difference remains constant, but the head in the closed tidal system varies very slowly. The relatively small-scale numerical simulation of varying outlet pressure for the nozzle with 10 inches inlet diameter and 5.75 inches outlet diameter shows that the static pressure difference remains constant to obtain the same velocity.

Furthermore, results show that the velocity at the nozzle outlet is consistent with the general concept of nozzle convergence and conservation of mass, i.e., mass flux is conserved through the nozzle. Still, the efficiency appears to decrease slightly with increasing outlet pressure. Table 5 showing the results for the varying outlet pressure is shown in Appendix 1. Power generation in the system is given by $\rho v^3 A$, which can be shown to be an increasing function of the degree of convergence. Thus, the ability of a constant static pressure differential to provide results, using a simple convergence ratio that is in good agreement with the detailed numerical model used here, is very important.

The nozzle with 10 inches outlet diameter and 5.75 inches inlet diameter displays the desired velocity of this system, i.e., approximately 10 m/s. Furthermore, the size of the mesh also plays a role in the accuracy of the results. The result between the fine mesh and the coarse mesh varies by 3%, which is shown in Table 6, and the volume rendering for different mesh sizes is shown in Appendix 3.

Future Work

The research requires more study and analysis of other aspects as it doesn't complete only with the optimization of the nozzle. Apart from nozzle optimization, some future works that need further study are as follows:

1. Modeling of the whole system in ANSYS.
2. The small-scale laboratory tests of the closed system. This will help to evaluate the performance of the whole system as well as the performance of the optimized nozzle. The results can be compared with the results obtained from the ANSYS FLUENT.

3. Once the size of the nozzle is optimized, the further step will be optimizing the location of the nozzle. Two possible locations are the outlet of the bladder and right before the turbine. Some tidal stations involve the installation of large underwater turbines in areas with high tidal movement so that they can capture the kinetic motion of the surging of ocean tides. Underwater turbines are prone to biofouling. Unlike tidal barrages and tidal stream generators, there would be no risk to marine wildlife if the turbine is placed onshore or within the bladder.
4. Investigation of the potential effect on the offshore area that may occur because of the presence of the bladder.
5. Selecting the type of turbine is also important. Different turbines have unique performance and efficiencies. It is significant to choose the turbine which delivers high efficiency. Moreover, the effect of different nozzles on the performance of the turbine should be analyzed.

9. Appendix 1

Table 4: Velocity and the inlet pressure of the nozzle with inlet diameter 12 inches and varying outlet diameters.

Inlet diameter of the nozzle (inches)	**Outlet diameter of the nozzle (inches)**	$\boldsymbol{C = \frac{D_{outlet}}{D_{inlet}}}$	**Outlet velocity of the nozzle (m/s)**	**Inlet pressure of the nozzle (Pascal)**	**Efficiency (%)**
12	12	1	3.22	35,030	14.8
	9	0.75	5.967	45,320	39.28
	6	0.5	12.83	111,100	74.08
	4	0.333	29.79	450,000	98.605

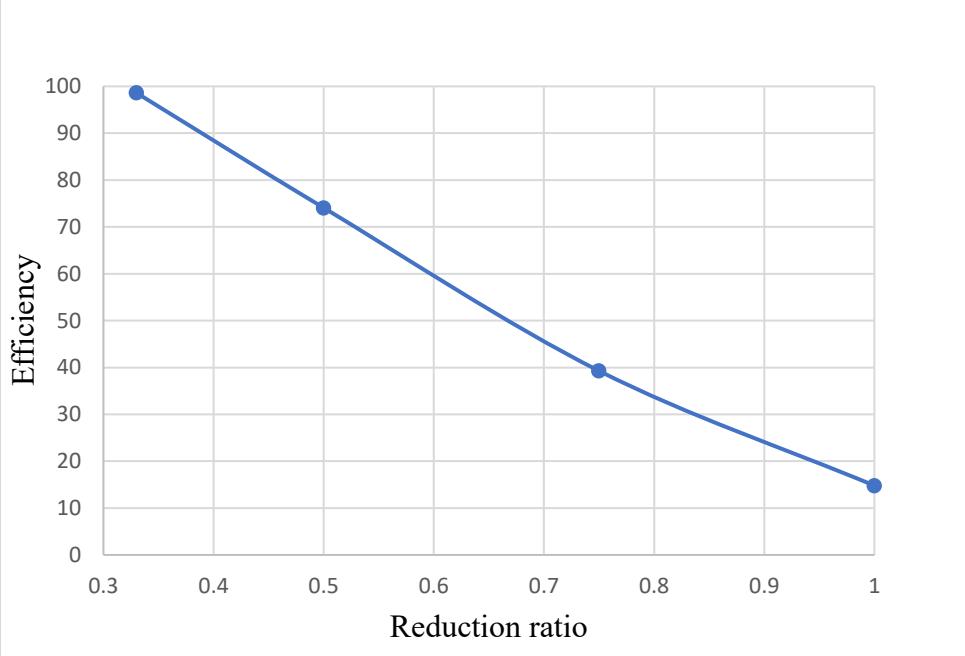

Figure 22: Graph between the reduction ratio and the efficiency of the nozzle.

Table 5: Comparision of the inlet pressures for various outlet pressures.

Outlet pressure of the nozzle (Pascal)	Inlet pressure of the nozzle from ANSYS (Pascal)	Pressure difference (Inlet pressure – outlet pressure)	Outlet velocity (m/s)	Efficiency (%)
10,000	5,2470	42,470	10.16	98.4
20,000	62,470	42,470	10.16	82.6
30,000	72,470	42,470	10.16	71.2
35,000	77,470	42,470	10.16	66.6
40,000	82,470	42,470	10.16	62.6
50,000	92,470	42,470	10.16	55.8

10. Appendix 2 (Mesh Sensitivity)

The velocity and pressure contour of the nozzle with inlet diameter 10 inches and outlet diameter 5.75 inches shown below for various meshing sizes.

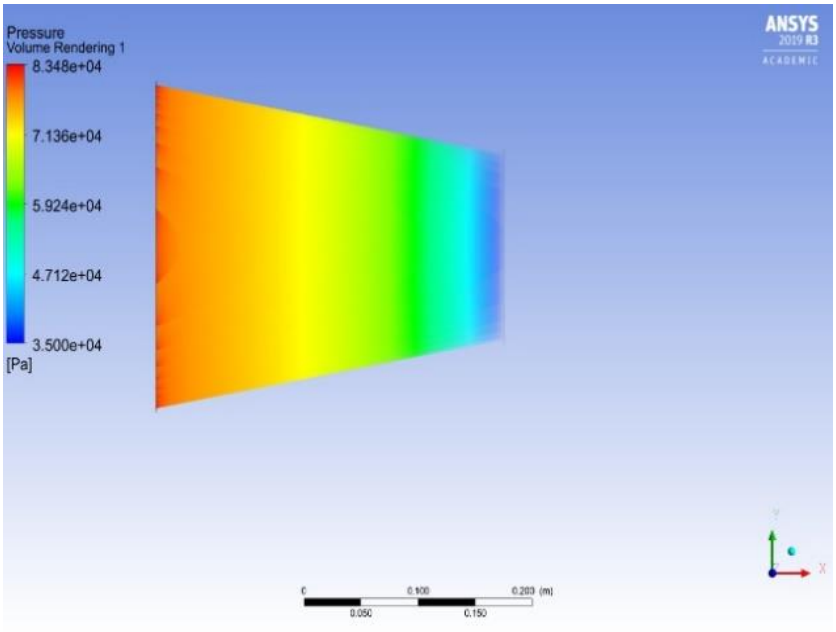

Figure 21: Pressure volume rendering for meshing size 0.001m

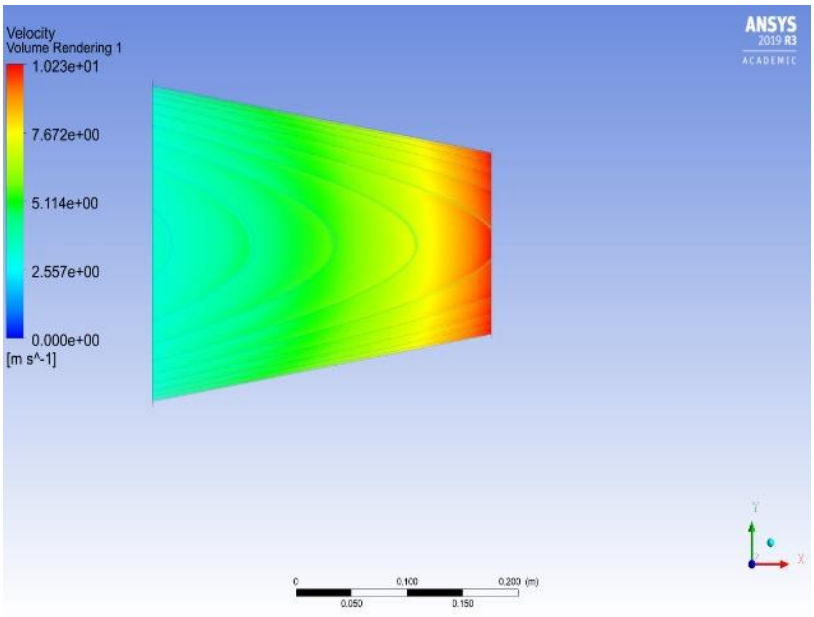

Figure 22: Velocity volume rendering for meshing size 0.001m

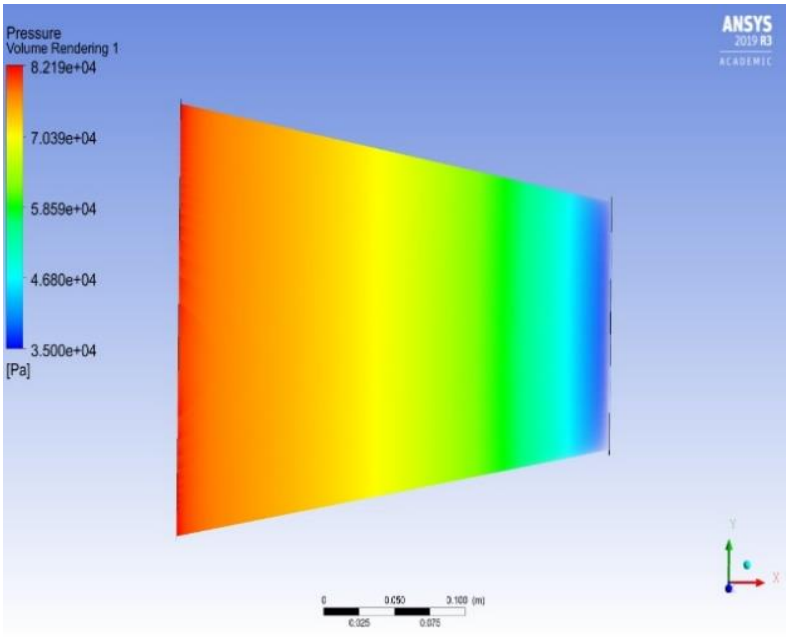

Figure 23: Pressure volume rendering for meshing size 0.002 m

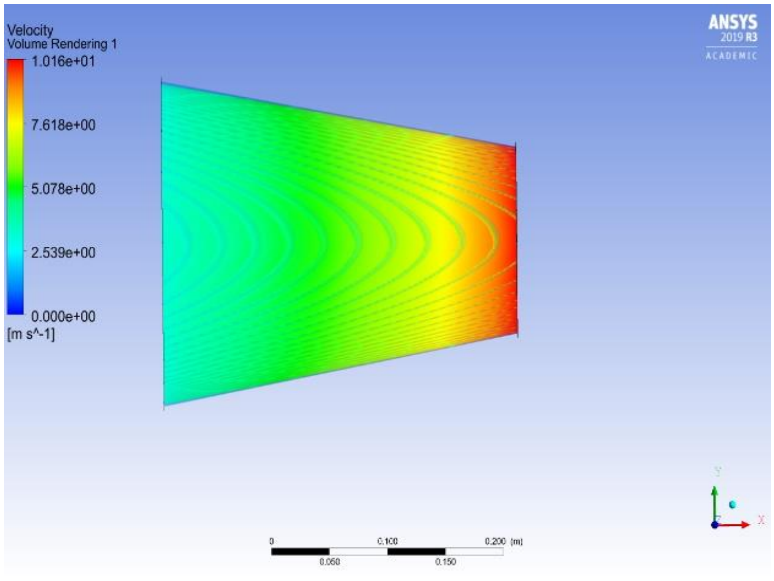

b

Figure 24: Velocity volume rendering for mesging size 0.002m

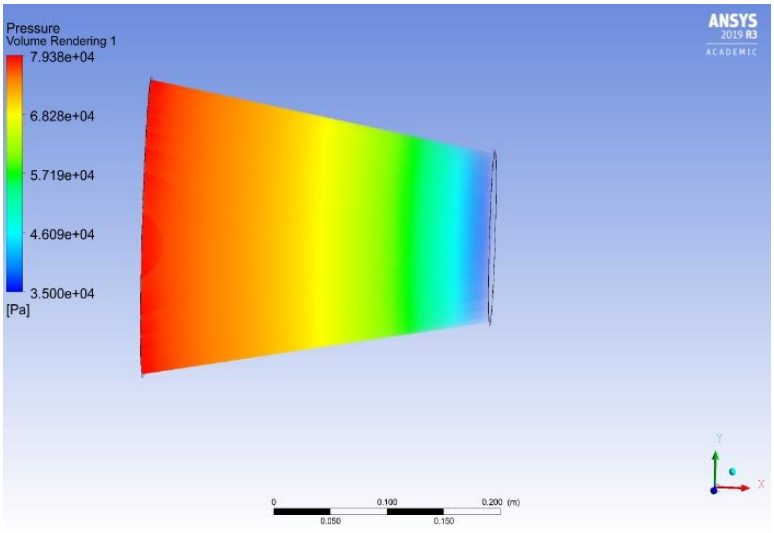

Figure 25: Pressure volume rendering for meshing size 0.008m

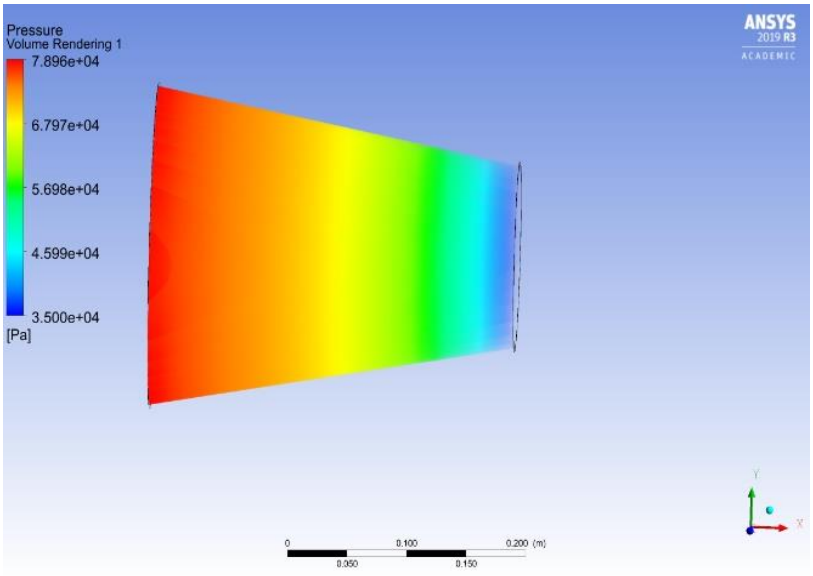

Figure 26: Pressure volume rendering for meshing size 0.01m

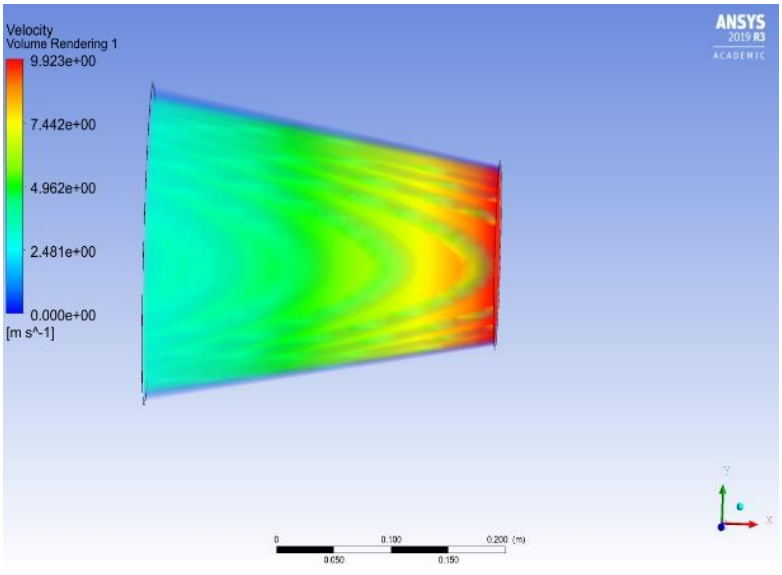

Figure 27: Velocity volume rendering for meshing 0.01m

Table 6: Velocity and Inlet pressure of the nozzle with inlet diameter 10 inch and outlet diameter 5.75 inch for different meshing size

Meshing element size (m)	**Velocity (m/s)**	**Pressure (Pascal)**
0.001	10.23	78,640
0.002	10.16	77,470
0.005	10.03	75,900
0.008	9.948	79,380
0.01	9.923	78,960

11. Appendix 3

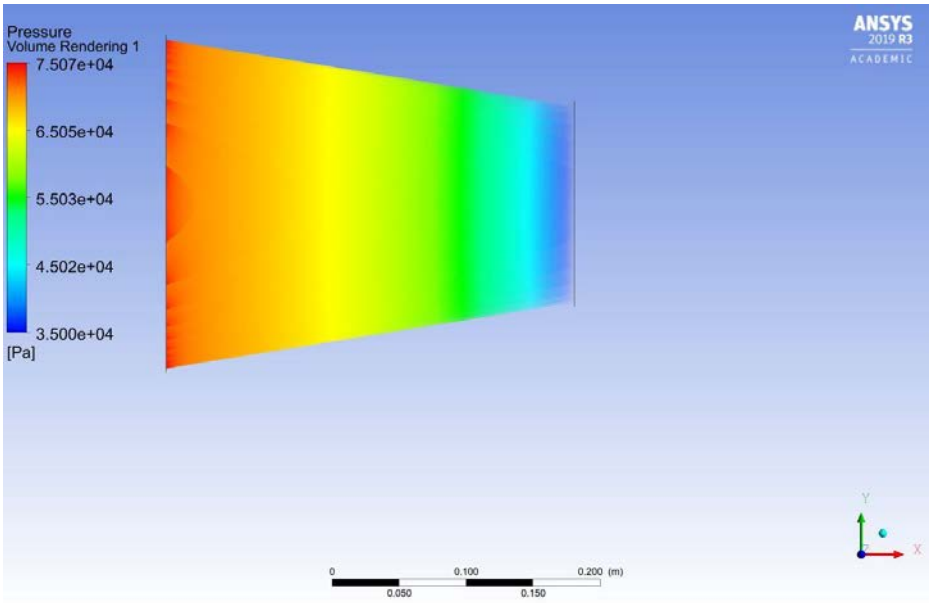

Figure 28: Pressure volume rendering for the nozzle with outlet diameter 6 inches

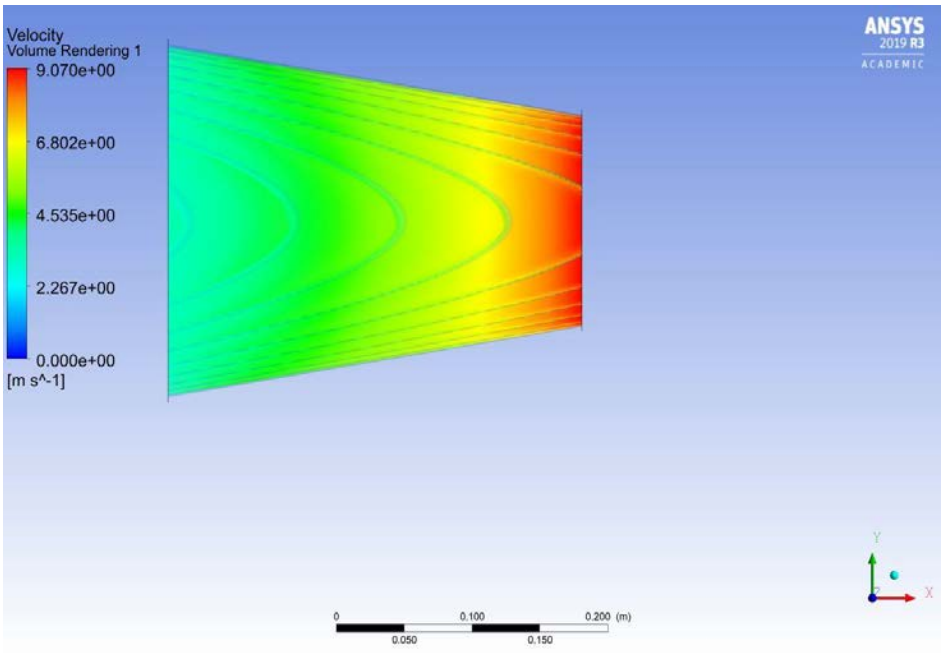

Figure 29: Velocity volume rendering for the nozzle with outlet diameter 6 inches

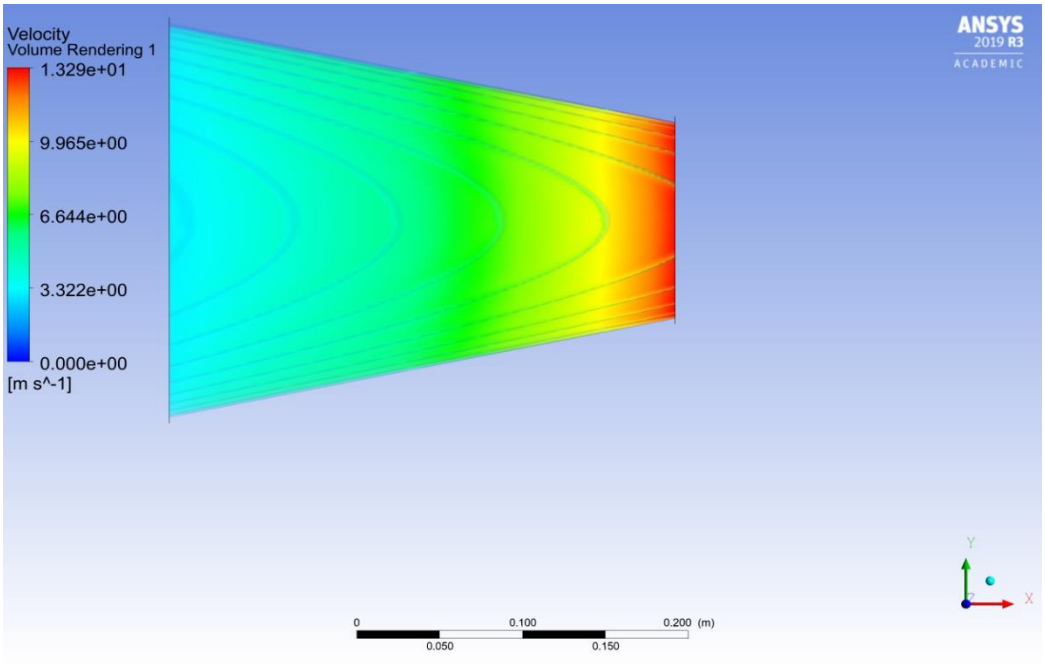

Figure 30: Velocity volume rendering of the nozzle with outlet diameter 5 inches

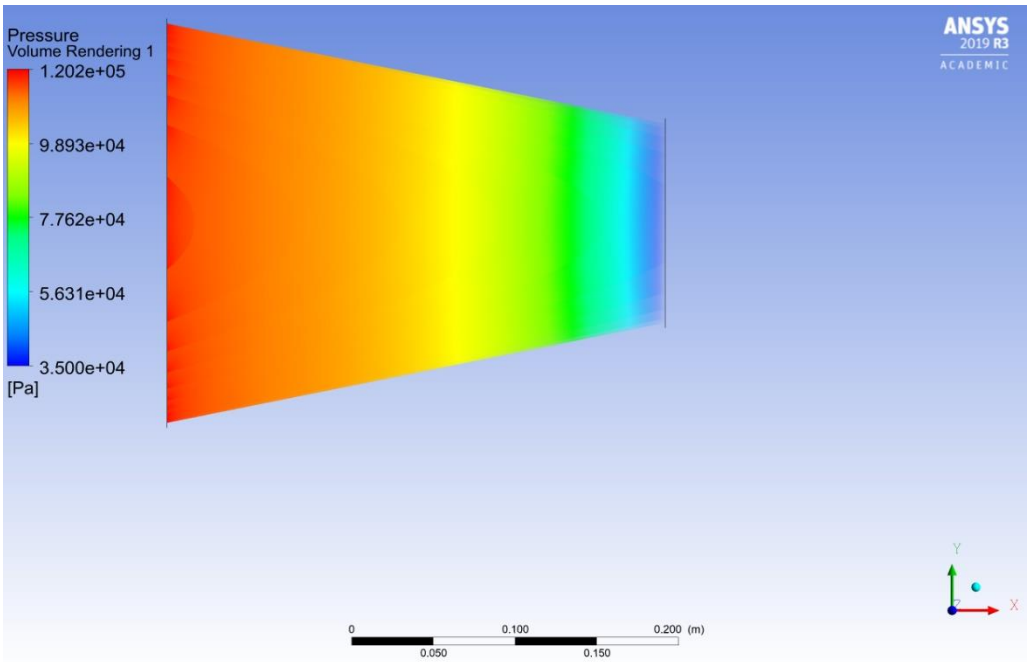

Figure 31: Pressure volume rendering of the nozzle with outlet diameter 5 inches

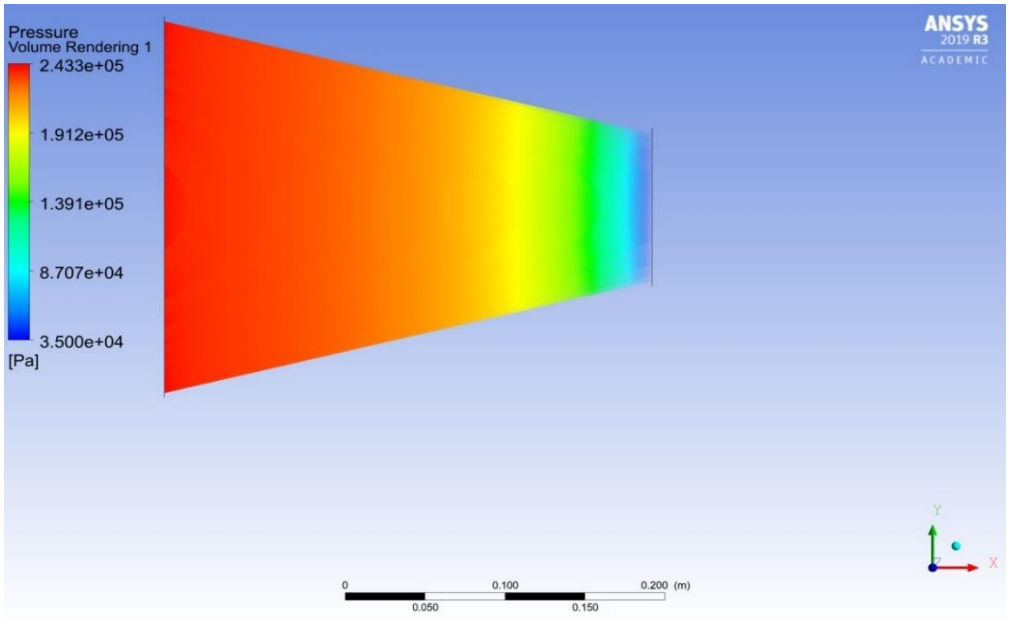

Figure 32: Pressure volume rendering for the nozzle with outlet diameter 4 inches

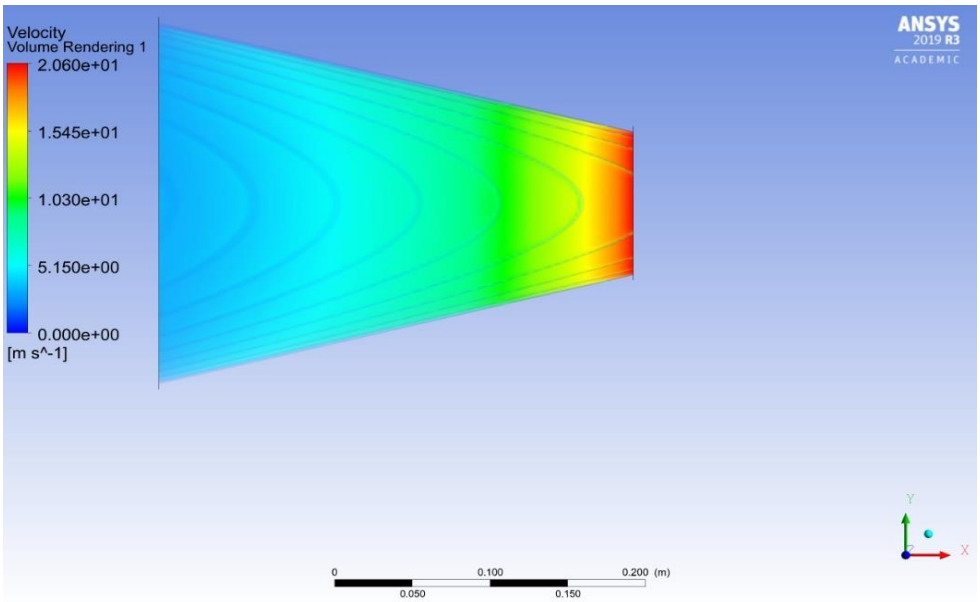

Figure 33: Velocity volume rendering for the nozzle with outlet diameter 4 inches

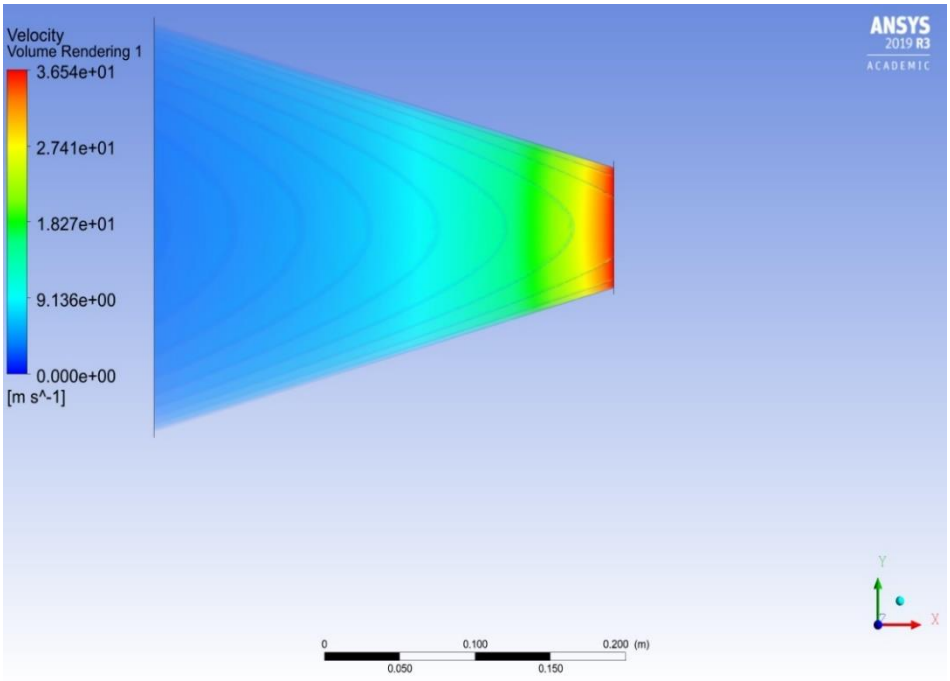

Figure 34: Velocity volume rendering of the nozzle with 3 outlet diameter 3 inches

12. References

1. Ali, T., Gupta, S. D., Arnab, I. Z., & Ferdous, S. M. (2012). An Analysis of the Potentiality of Tidal Power in Sandwip by Using One Way & Two-Way Power Generation Technology: An Ideal Model. *International Journal of Renewable Energy Research (IJRER)*, *2*(3), 535-540.
2. Ahmed, S., Riaz, R., & Anwar, M. (2016). Utilization of Water Flow in Existing Canal System for Power Generation Through Flow Acceleration Using Converging Nozzles. *American Journal of Engineering Research (AJER), 5,*115-123.
3. Budiyanto, M. A., Novri, J., Alhamid, M. I., & Ardiyansyah. (2019). Analysis of Convergent and Divergent-Convergent Nozzle of Waterjet Propulsion by CFD Simulation. *AIP Conference Proceedings*, *2062*(1), 020066-1.
4. Dixon, A., & Watt, T. (2017). Swansea Bay Tidal Lagoon Power Plant - a world first. *Civil Engineering (10212000)*, *25*(7), 15–20.
5. (EIA), U. E. (2017, September 14). *International Energy Outlook 2017 - EIA*. Retrieved from US Energy Information Administration: https://www.eia.gov › outlooks › ieo › pdf › 0484(2017)
6. (EIA), U. E. (2019, September 23). *Tidal Power*. Retrieved from US Energy Information Administration (EIA): https://www.eia.gov › energyexplained › hydropower › tidal-power
7. Elbatran, A. H., Yaakob, O. B., Ahmed, Y. M., & Shabara, H. M. (2015). Numerical study for the use of different nozzle shapes in microscale channels for producing clean energy. *International Journal of Energy and Environmental Engineering*, *6*(2), 137-146.
8. Etemadi, A., Emami, Y., AsefAfshar, O., & Emdadi, A. (2011). Electricity generation by the tidal barrages. *Energy Procedia*, *12*, 928-935.

9. Geographic, N. (2011). *Tidal energy*. Retrieved from National Geographic: nationalgeographic.org/encyclopedia/tidal-energy

10. Khan, A. A., Khan, A. M., Zahid, M., & Rizwan, R. (2013). Flow acceleration by converging nozzles for power generation in existing canal system. *Renewable energy*, *60*, 548-552.

11. Khare, V., Khare, C., Nema, S., & Baredar, P. (2018). *Tidal Energy Systems: Design, Optimization and Control*. Elsevier.

12. Kim, Y. H. (2016, August 2). *Technology case study: Sihwa Lake tidal power station*. Retrieved from International Hydropower Association - Advancing sustainable hydropower: https://www.hydropower.org/blog/technology-case-study-sihwa-lake-tidal-power-station.

13. Lovejoy, D. W. (2018). Tidal energy. *Salem Press Encyclopedia*.

14. Montllonch Araquistain, T. (2010). Tidal Power: Economic and Technological Assessment.

15. NOAA. (2001, february). *Tidal Datums and Their Applications*. Retrieved from https://tidesandcurrents.noaa.gov/publications/tidal_datums_and_their_applications.pdf

16. Neill, S. P., Angeloudis, A., Robins, P. E., Walkington, I., Ward, S. L., Masters, I., ... & Aggidis, G. (2018). Tidal range energy resource and optimization–Past perspectives and future challenges. *Renewable energy*, *127*, 763-778.

17. Patel, K. (2019). Prospective of Tidal Energy.

18. Petley, S., & Aggidis, G. (2016). Swansea Bay tidal lagoon annual energy estimation. *Ocean Engineering*, *111*, 348-357.

19. Rourke, F. O., Boyle, F., & Reynolds, A. (2010). Tidal energy update 2009. *Applied energy*, *87*(2), 398-409.

20. SciJinks. (2019, November 13). *NOAA SciJinks*. Retrieved from SciJinks: https://scijinks.gov/tides/

21. Selin, N. E. (2019, April 04). *Tidal Power*. Retrieved from Encyclopædia Britannica: https://www.britannica.com/science/tidal-power

22. Srinivas, G., & Rakham, B. (2017, May). Experimental and numerical analysis of convergent nozzlex. In *IOP Conference Series: Materials Science and Engineering* (Vol. 197, No. 1, p. 012081). IOP Publishing.

23. Sumich, J., Thurman, H., & Ross, D. *Tides and water level.* Retrieved from National ocean service: https://oceanservice.noaa.gov/education/tutorial_tides/tides02_cause.html.

24. Tafreshi, H. V., & Pourdeyhimi, B. (2003). Simulating the flow dynamics in hydroentangling nozzles: effect of cone angle and nozzle aspect ratio. *Textile research journal*, *73*(8), 700-704.

25. Tech, G. (2011). Assessment of energy production potential from tidal streams in the U.S. *Georgia Tech Research, Atlanta, GA,(http://www1. eere. energy. gov/water/pdfs/1023527. pdf) (Mar. 2013)*.

26. Todeschini, G. (2017). Review of tidal lagoon technology and opportunities for integration within the UK energy system. *Inventions*, *2*(3), 14.

27. Tousif, S. M. R., & Taslim, S. M. B. (2011). Tidal power: an effective method of generating power. *International Journal of Scientific & Engineering Research*, *2*(5), 1-5.

28. Van Haren, H. (2010). Tidal power? No thanks. *New Scientist*, *206*(2754), 20–21. https://doi.org/10.1016/S0262-4079(10)60780-4
29. Vieira, M. A. (2018). An Integrated Closed Convergent System for Optimal Extraction of Head-Driven Tidal Energy.
30. Wang, C., He, X., Cheng, L., Luo, C., Xu, J., Chen, K., & Jiao, W. (2019). Numerical Simulation on Hydraulic Characteristics of Nozzle in Waterjet Propulsion System. *Processes*, *7*(12), 915.
31. Waters, S., & Aggidis, G. (2016). A world first: Swansea Bay tidal lagoon in review. *Renewable and Sustainable Energy Reviews*, *56*, 916-921.
32. Wemyss, M. H. (2014). *Relational development site appraisal model for the deployment of Marine Energy Convertors in Scotland* (Doctoral dissertation, Heriot-Watt University).
33. Yu, Y., Shademan, M., Barron, R. M., & Balachandar, R. (2012). CFD study of effects of geometry variations on flow in a nozzle. *Engineering applications of computational fluid mechanics*, *6*(3), 412-425.
34. Watanawanavet, S. (2005). *Optimization of a high-efficiency jet ejector by computational fluid dynamic software* (Doctoral dissertation, Texas A&M University).
35. Singh, J., Zerpa, L. E., Partington, B., & Gamboa, J. (2019). Effect of nozzle geometry on critical-subcritical flow transitions. *Heliyon*, *5*(2), e01273. https://doi.org/10.1016/j.heliyon.2019.e01273
36. Ghassemieh, E., Versteeg, H. K., & Acar, M. The Effect of Nozzle Geometry on the Flow Characteristics of Small Water Jets.
37. Zainol, M. Z., Ismail, N., Zainol, I., Abu, A., & Dahalan, W. (2017). A review on the status of tidal energy technology worldwide. *Sci. Int*, *29*, 659-667.

38. (n.d.). Retrieved from Tethys: https://tethys.pnnl.gov/project-sites/la-rance-tidal-barrage

39. (n.d.). Retrieved from EDF: https://www.edf.fr/en/the-edf-group/industrial-provider/renewable-energies/marine-energy/tidal-power

40. (2014, November 7). Retrieved from Business Green: https://www.businessgreen.com/bg/feature/2379437/the-worlds-10-biggest-tidal-power-plants

Thank You